COLLAGE 2023

Lecture 09: Ionosphere Observation with Radio Waves

Yang Wang

Smead Department of Aerospace Engineering Sciences

University of Colorado Boulder

Email: yang.wang-2@colorado.edu

Source materials partially from Jade Morton and Robert Marshall

Outline

- **Overview of ionosphere observation approaches**
- **GNSS network-based ionosphere observation and monitoring**
- **GNSS space-based ionosphere observations**

Ionosphere Irregularities: Temporal Evolution

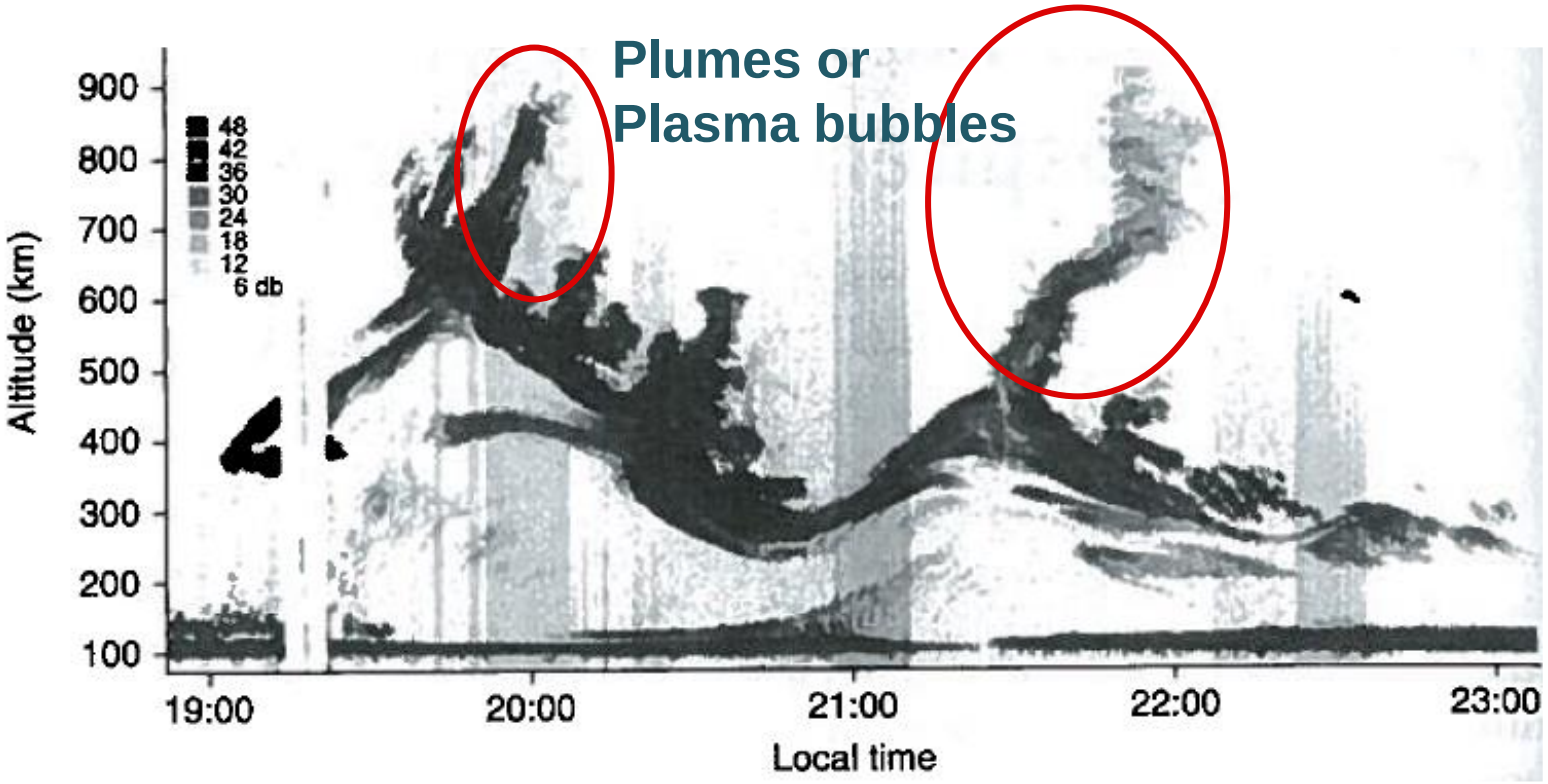

Jicamarca, Peru, vertical backscatter at 3m
3/21/1979

Kelley, M. C., Larsen, M. F., LaHoz, C.A., and McClure, J. P., “Gravity wave of equatorial spread F: A case study,” J. Geophys. Res, 86, p9087, 1981.

- Electron Density
- Ion and Electron Temperature
- Ion Drift
- Ionospheric Composition

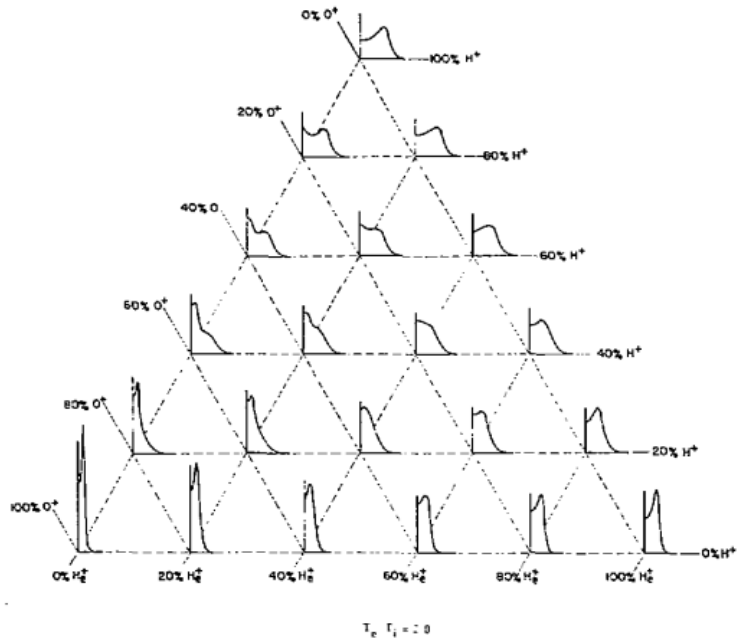

Fig. 2—Spectra for mixtures of O^+, H_e^+, and H^+.

Gordon, 1964

World incoherent scatter radars

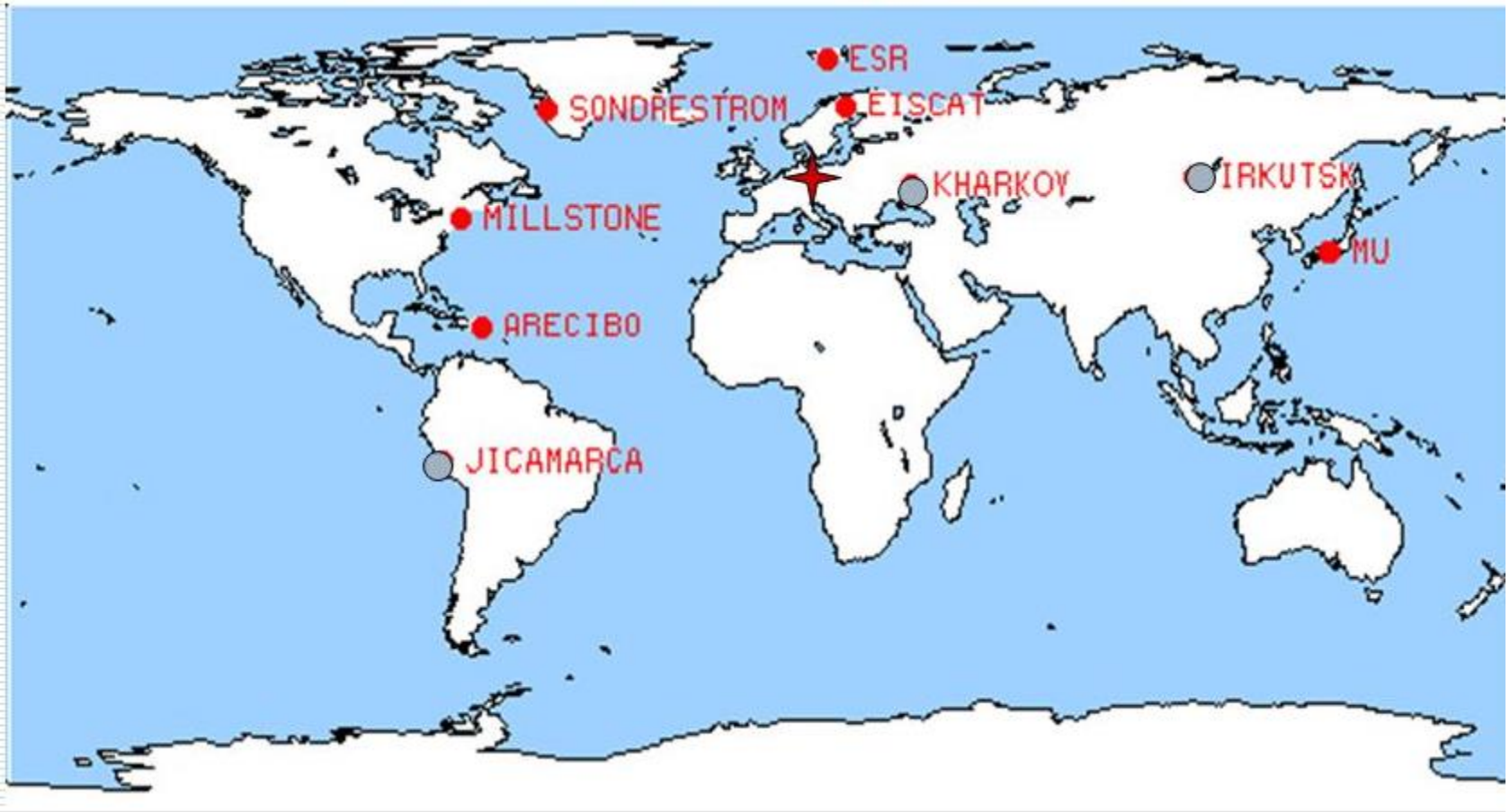

Ionosphere Irregularity: Vertical Structure

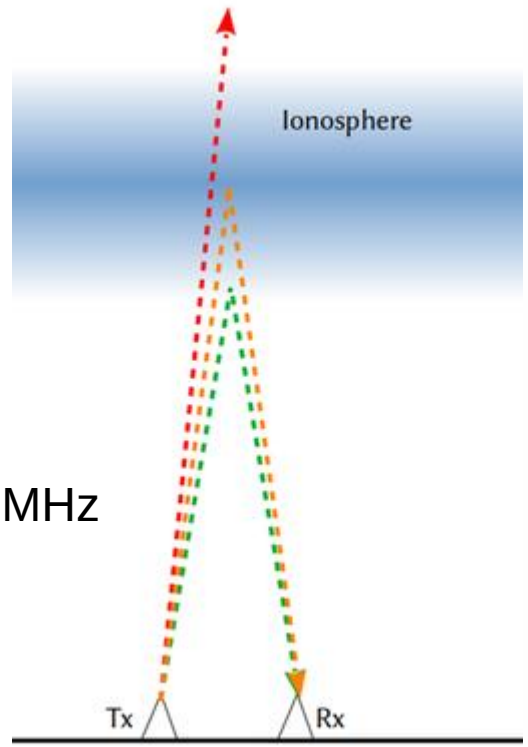

Ionosonde

HF typically 0.5–23 MHz
or 1–40 MHz

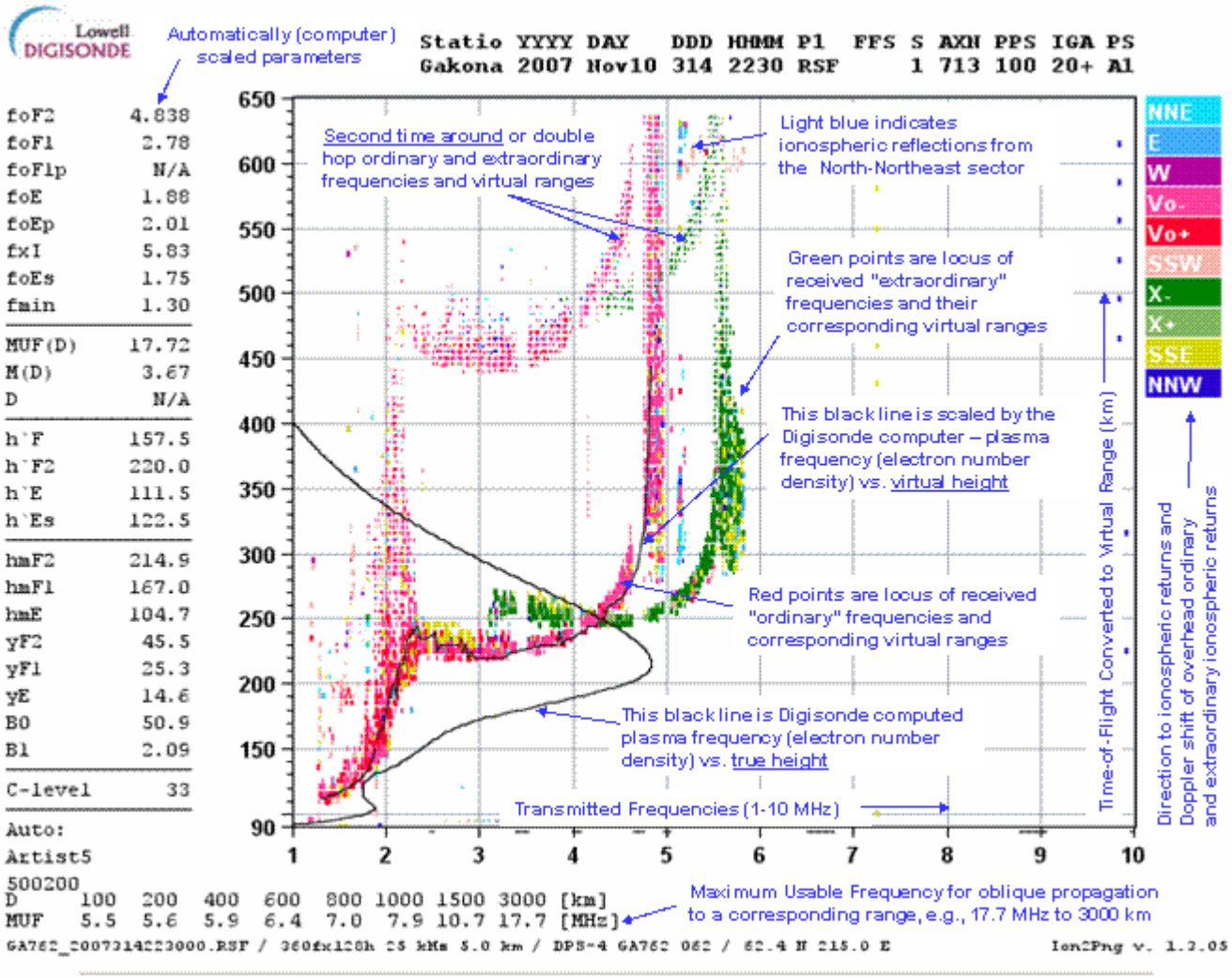

Ionosphere Irregularity: Vertical Structure

Altair radar on Kwajalein island 0.96m wavelength

PLUMEX I rocket

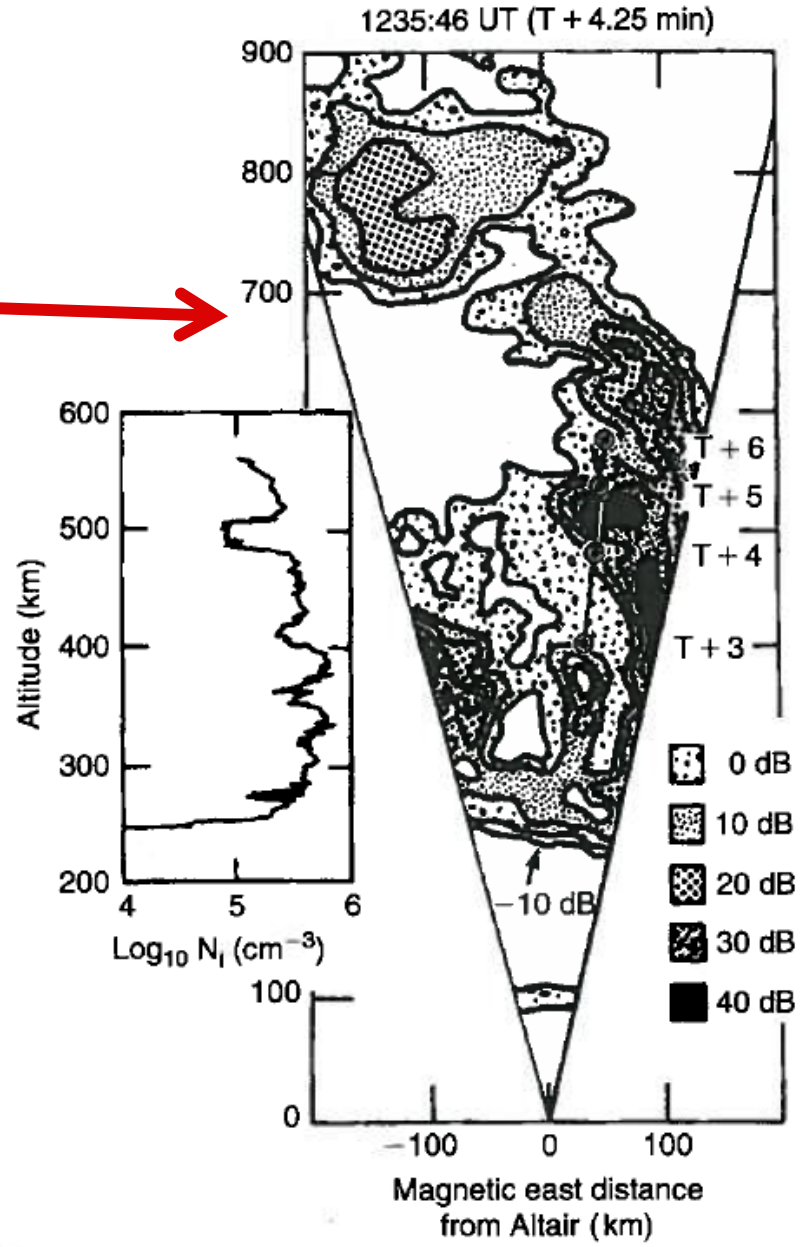

Rino, Tsunoda, Petriceks, Livingston, Kelley, Baker, “Simultaneous rocket-borne beacon and in situ measurements of equatorial spread F – intermediate wavelength results,” J. Geophys. Res., 86(4), p2411, 1981.

Ionosphere Irregularity: Horizontal Structure

AE-E satellite →

Altair radar →

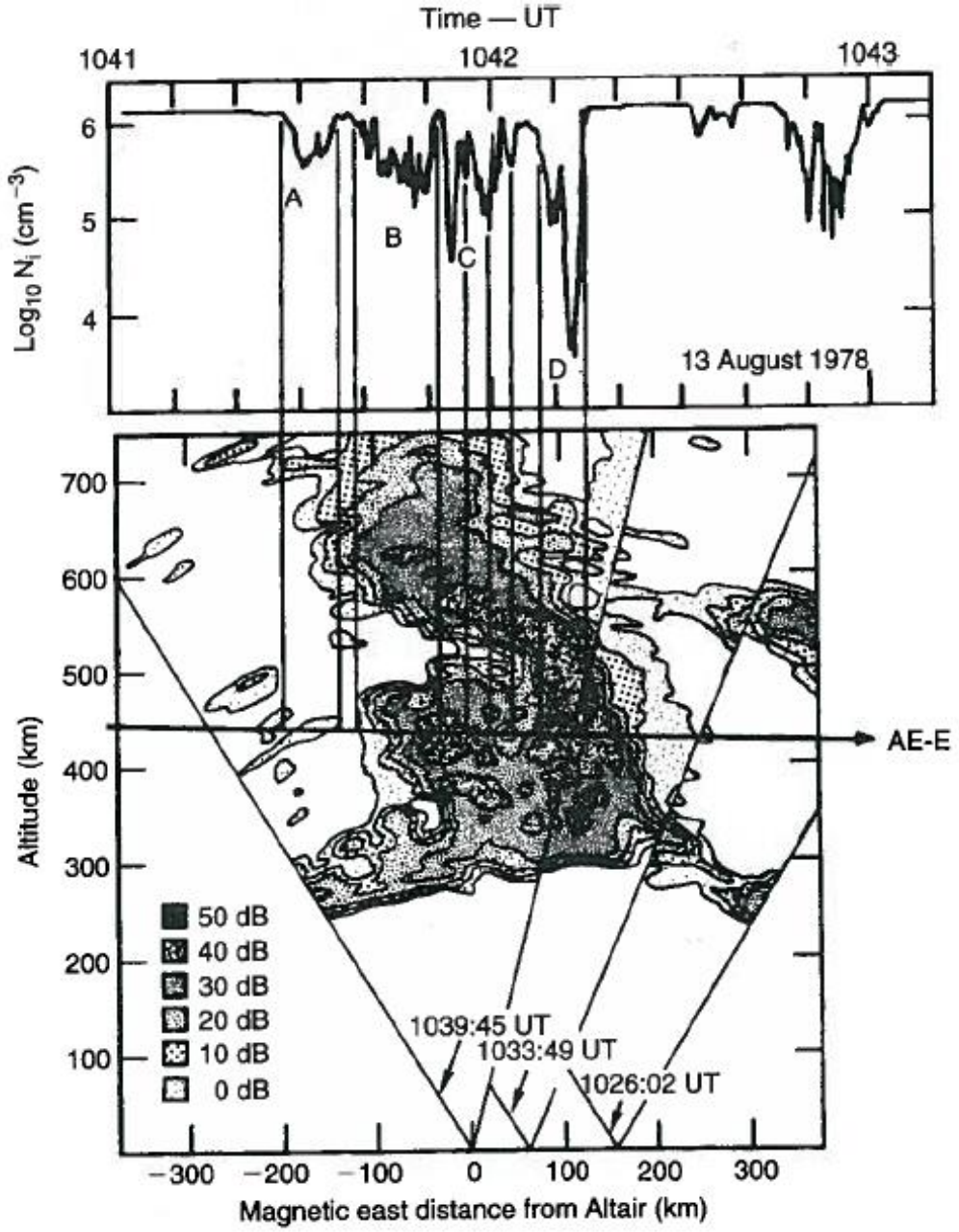

Tsunoda, Livingtons, McClure, Hanson, "Equatorial plasma bubbles: vertically elongated wedges from the bottomside F layer," J. Geophys. Res., 87, p9171, 1982.

NASA's Ionospheric Connection Explorer (ICON)

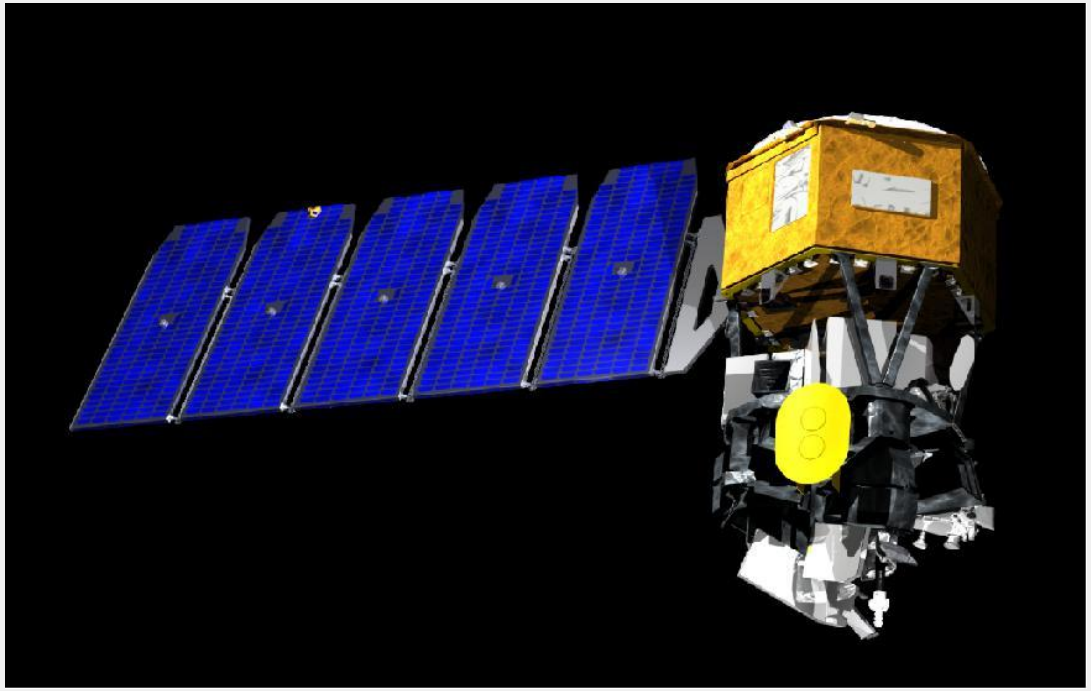

- Main instruments:
  - **MIGHTI** is a Michelson Interferometer to measure winds and temperatures
  - **FUV** is an FUV imager; observes UV emissions of N_2 and O to determine O/N_2 ratio
  - **EUV** images 83.4 nm emission from O; resonantly scattered by O+: gives ion density
  - **IVM** is the ion velocity meter; uses a Retarded Potential Analyzer (RPA) to measure relative velocity of ions, therefore winds, as well as temperature and density

- Understand drivers of ionospheric variability
- Explain how energy / momentum from lower atmosphere reach the space environment
- Explain how drivers create extreme conditions observed during solar-driven geomagnetic storms

GNSS Networks

IGS Global Ionosphere Map (GIM)

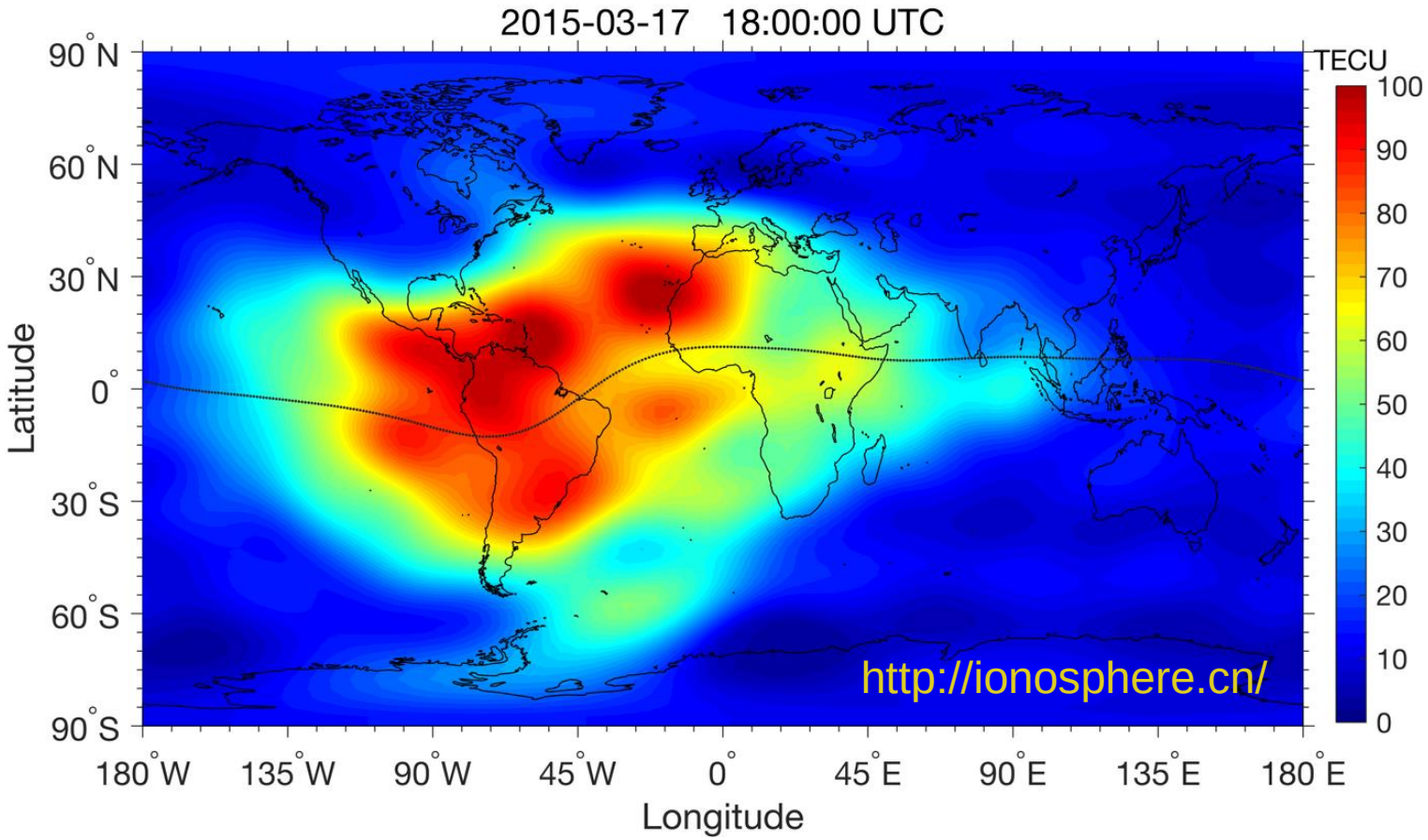

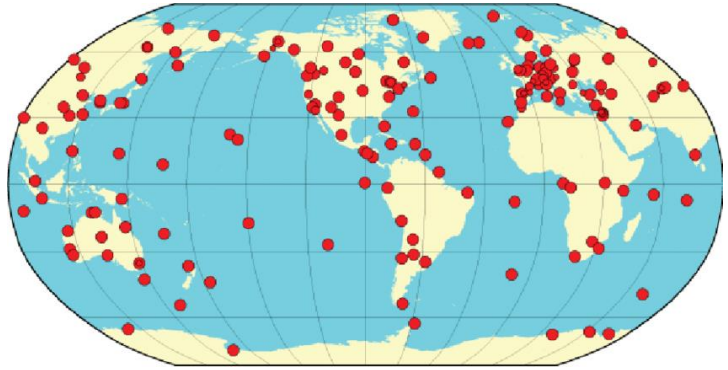

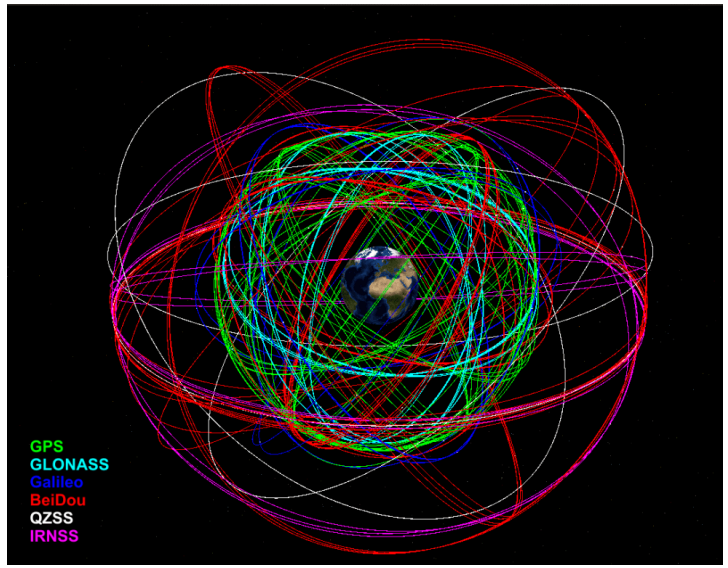

Outline

- Overview of ionosphere observation approaches
- **GNSS network-based ionosphere observation and monitoring**
- GNSS space-based ionosphere observations

Simplified Appleton-Hartree Equation

$$f_g \approx 1MHz \qquad f_p \leq 10MHz$$

At GPS frequency, $f \sim$ GHz: $\quad X = \left(\frac{f_p}{f}\right)^2 \ll 1 \qquad Y = \frac{f_g}{f} \ll 1$

$$n_\phi = 1 - \frac{X}{1 - \frac{Y^2 \sin^2\theta_B}{2(1-X)} \pm \sqrt{\frac{Y^4 \sin^4\theta_B}{4(1-X)^2} + Y^2\cos^2\theta_B}}$$

$$n_\phi \approx \underbrace{1}_{\text{Vacuum}} - \underbrace{\frac{X}{2}}_{1^{st}\text{ order}} \pm \underbrace{XY\left|\cos\theta_B\right|}_{2^{nd}\text{ order}} - \underbrace{\frac{1}{4}X\left(\frac{X}{2} + Y^2\left(1+\cos^2\theta_B\right)\right)}_{3^{rd}\text{ order}}$$

$$n_j \gg 1 - \frac{X}{2} \gg 1 - \frac{e^2}{2m\epsilon_0 f^2}N_e = 1 - 40.3\frac{N_e}{f^2}$$

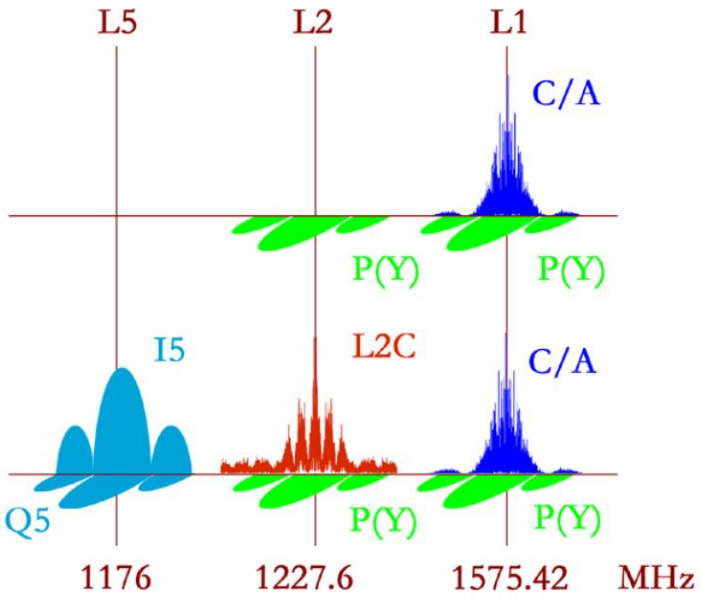

Ionosphere Disturbance Impact on Mid-latitudes

ROTI: Ionosphere Plasma Disturbance

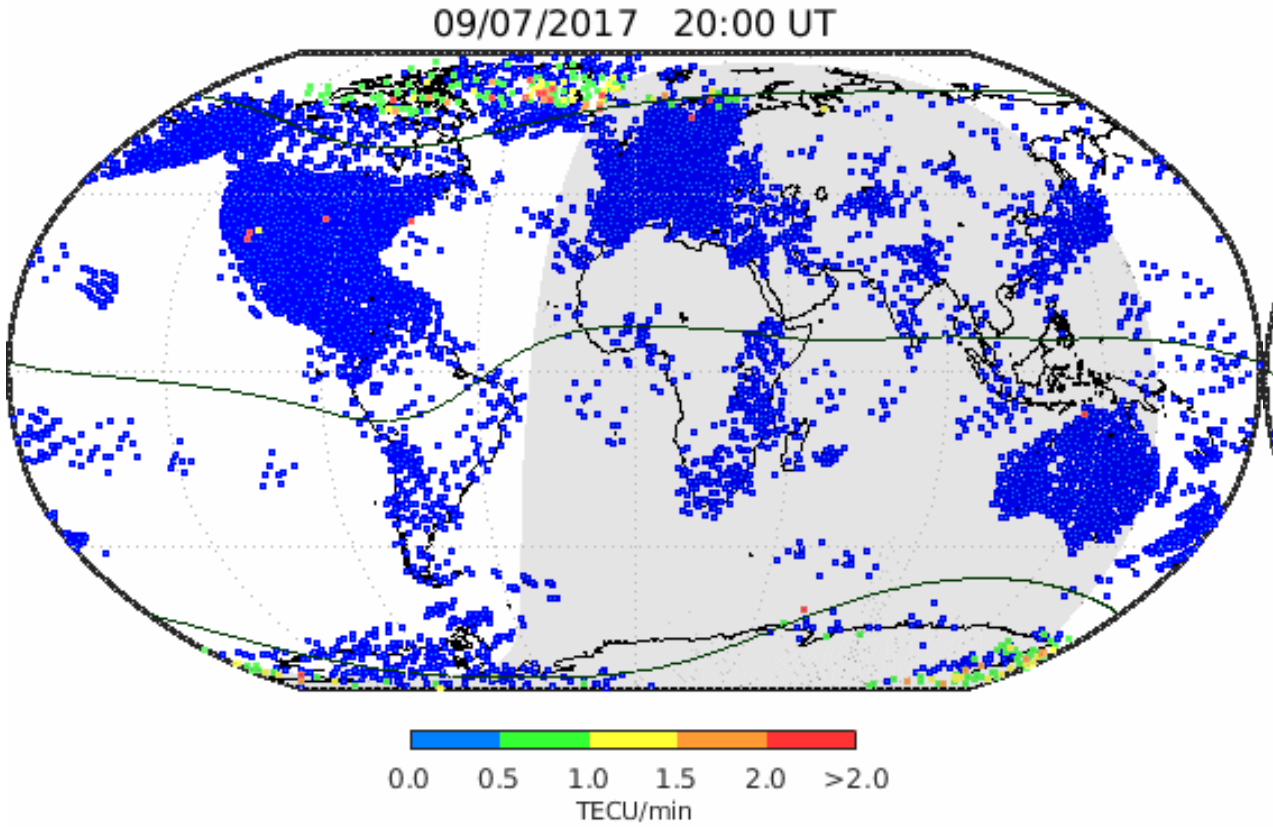

Position errors

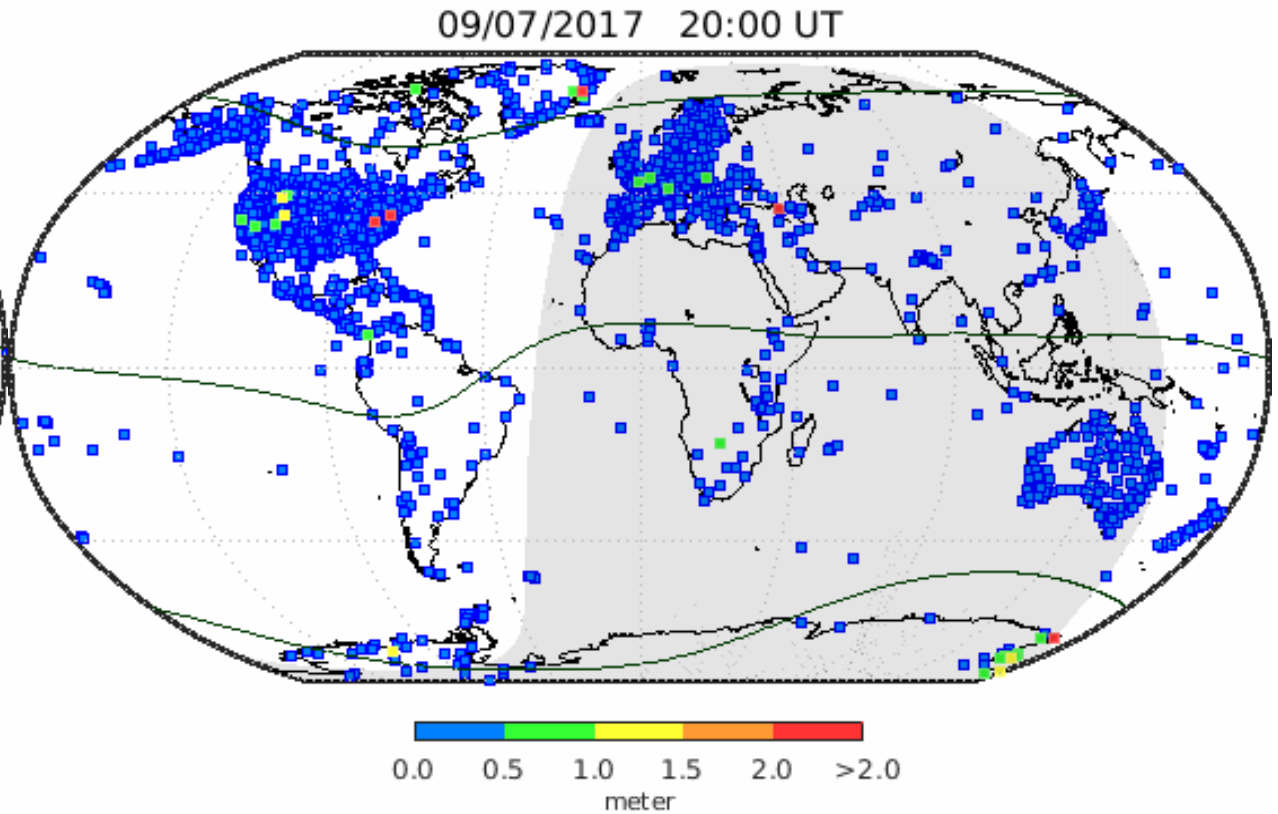

Yang, Z., S. Mrak, Y. Morton, "Geomagnetic storm induced mid-latitude ionospheric plasma irregularities and their implications for GPS positioning over North America: a case study," *Proc. IEEE/ION PLANS meeting*, 2020.

Challenges in Measuring Ionospheric Irregularities

1. Availability

Receivers cease to function if GNSS signal traverse irregularities
→ Data are not available when needed most!

2. Accuracy

$$(Iono + other) \otimes h(t) = Observed\ Effects$$

$$Iono\ \text{effects} \neq Observed\ Effects$$

Availability Issue: March 17-18, 2015 St. Patrick's Day storm

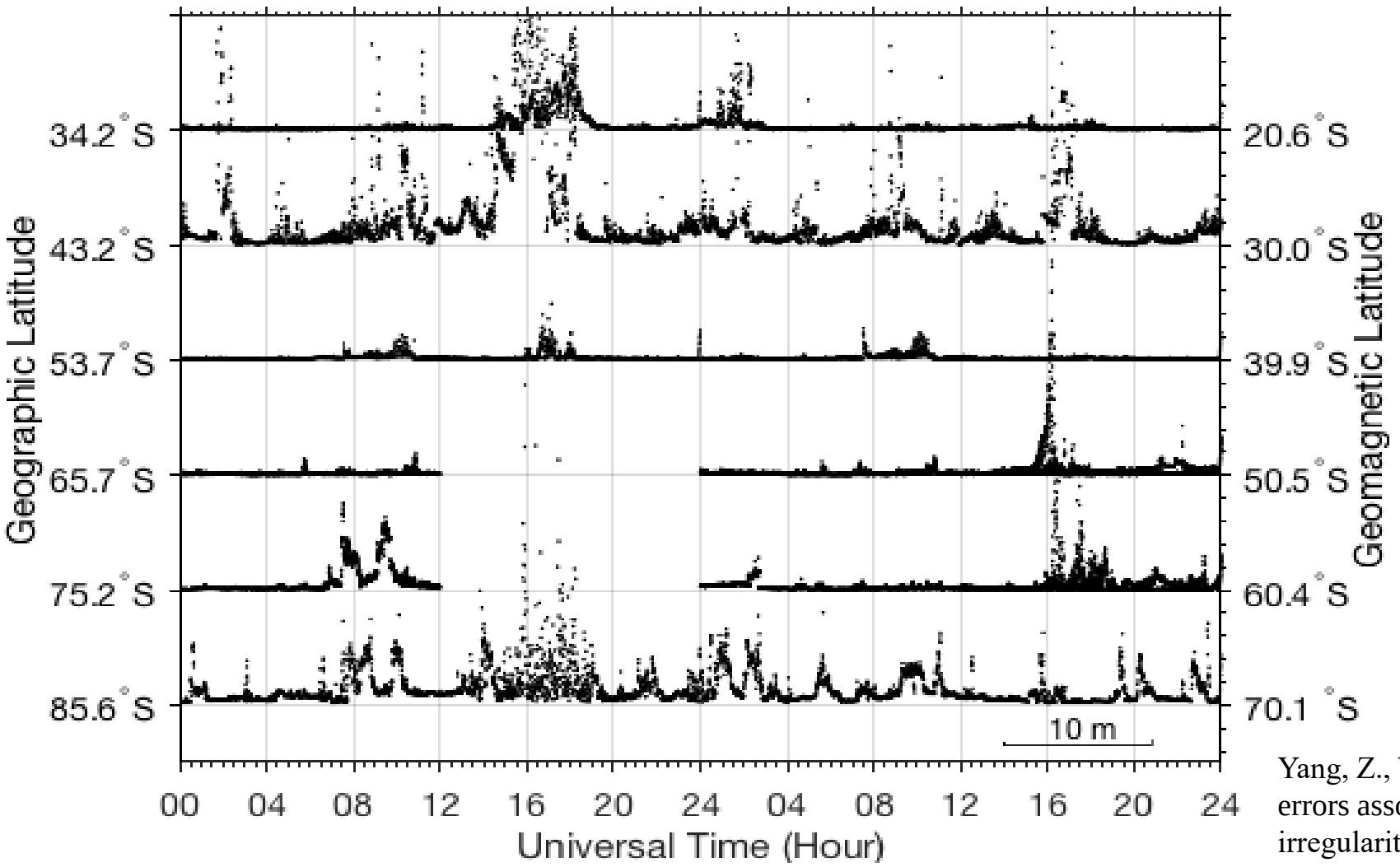

Yang, Z., Y. Morton, "Kinematic PPP errors associated with ionospheric plasma irregularities during the 2015 St. Patrick's day storm," *Proc. ION GNSS+*, 2019.

Accuracy: Scintillation Indices

Phase scintillation index: $\sigma_\phi = std\left(detrend\left(\phi_{s,k}\right)\right)$

Amplitude scintillation index: $S_4 = \sqrt{\dfrac{\langle SI^2\rangle - \langle SI\rangle^2}{\langle SI\rangle^2}}$

Signal intensity (power): $SI = \dfrac{SI_{raw}}{SI_{trend}}$ $\quad SI_{raw} = NBP - WBP$

Narrowband power: $NBP = \left(\sum_{i=1}^{M} I_i\right)^2 + \left(\sum_{i=1}^{M} Q_i\right)^2$

Wideband power: $WBP = \sum_{i=1}^{M} I_i^2 + \sum_{i=1}^{M} Q_i^2$

M: number of correlation blocks over a selected period
Typical setting: T_I =1ms → M=20; T_I =10ms → M=2

Rate of TEC Index (ROTI): $ROTI = \sqrt{E\left[\dfrac{|TEC(t+\delta t) - TEC(t)|^2}{\delta t^2}\right]}$

Global SDR Data Collection Network

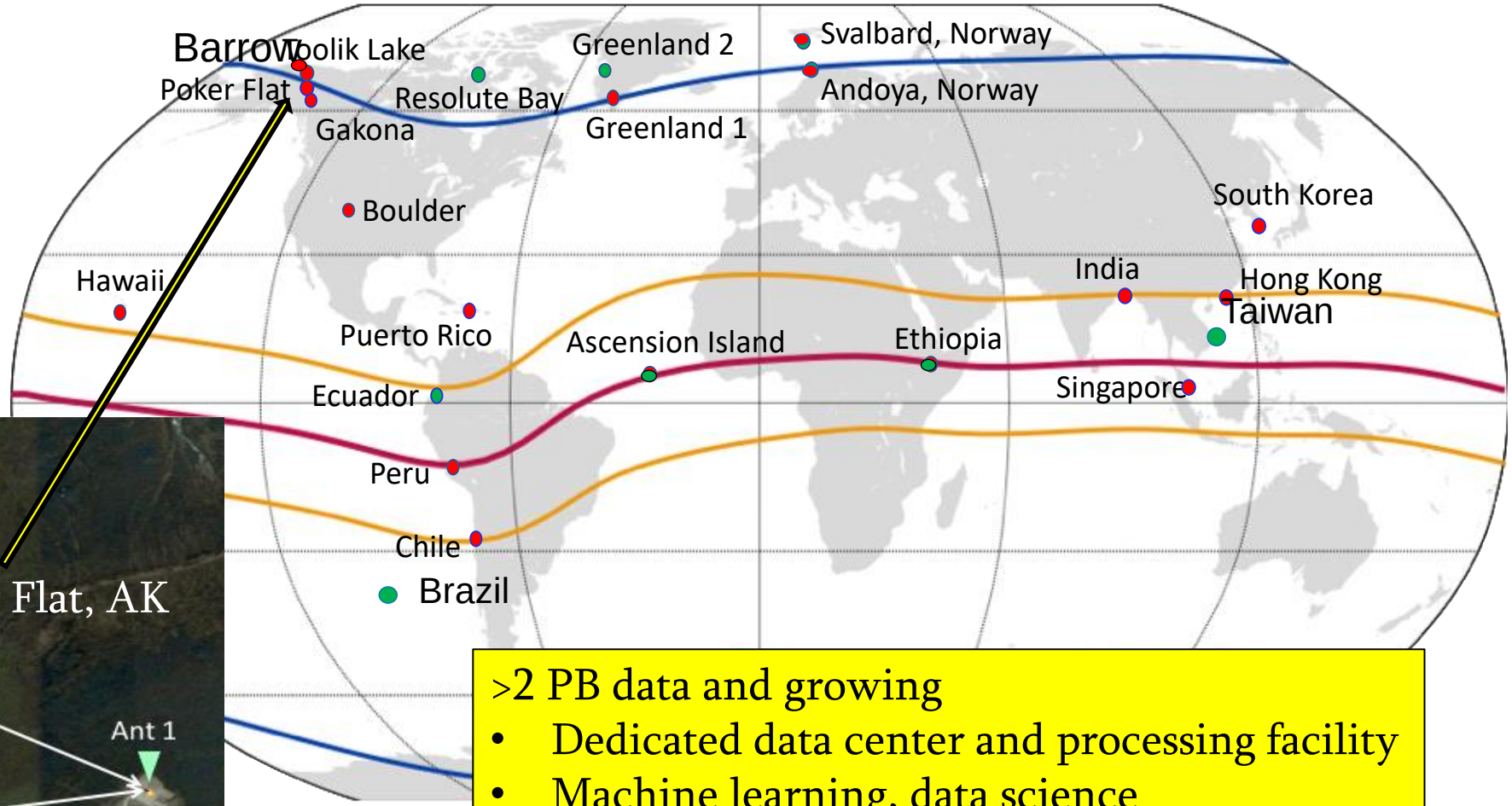

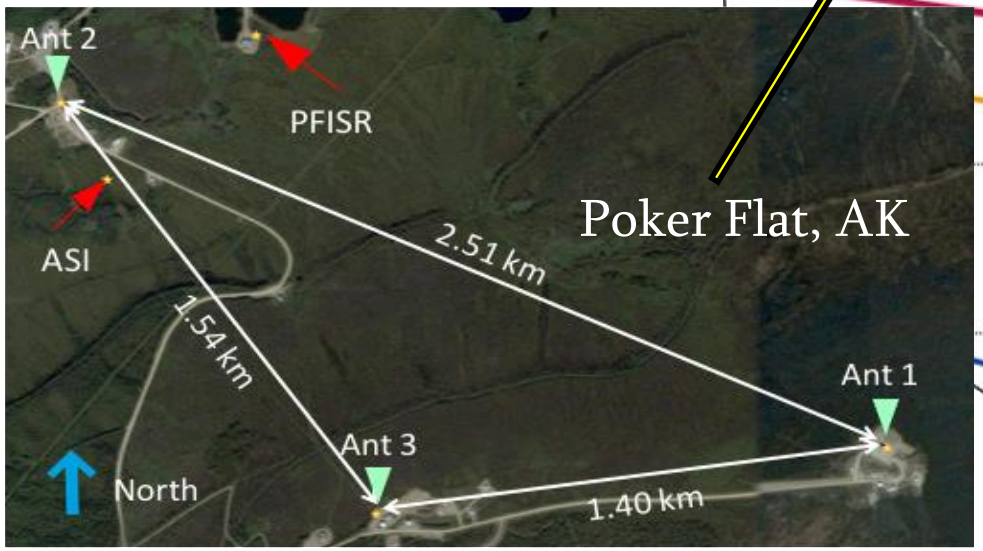

>2 PB data and growing

- Dedicated data center and processing facility
- Machine learning, data science

Low Latitude Scintillation Example

Peru
3/11/2013
13:30UTC

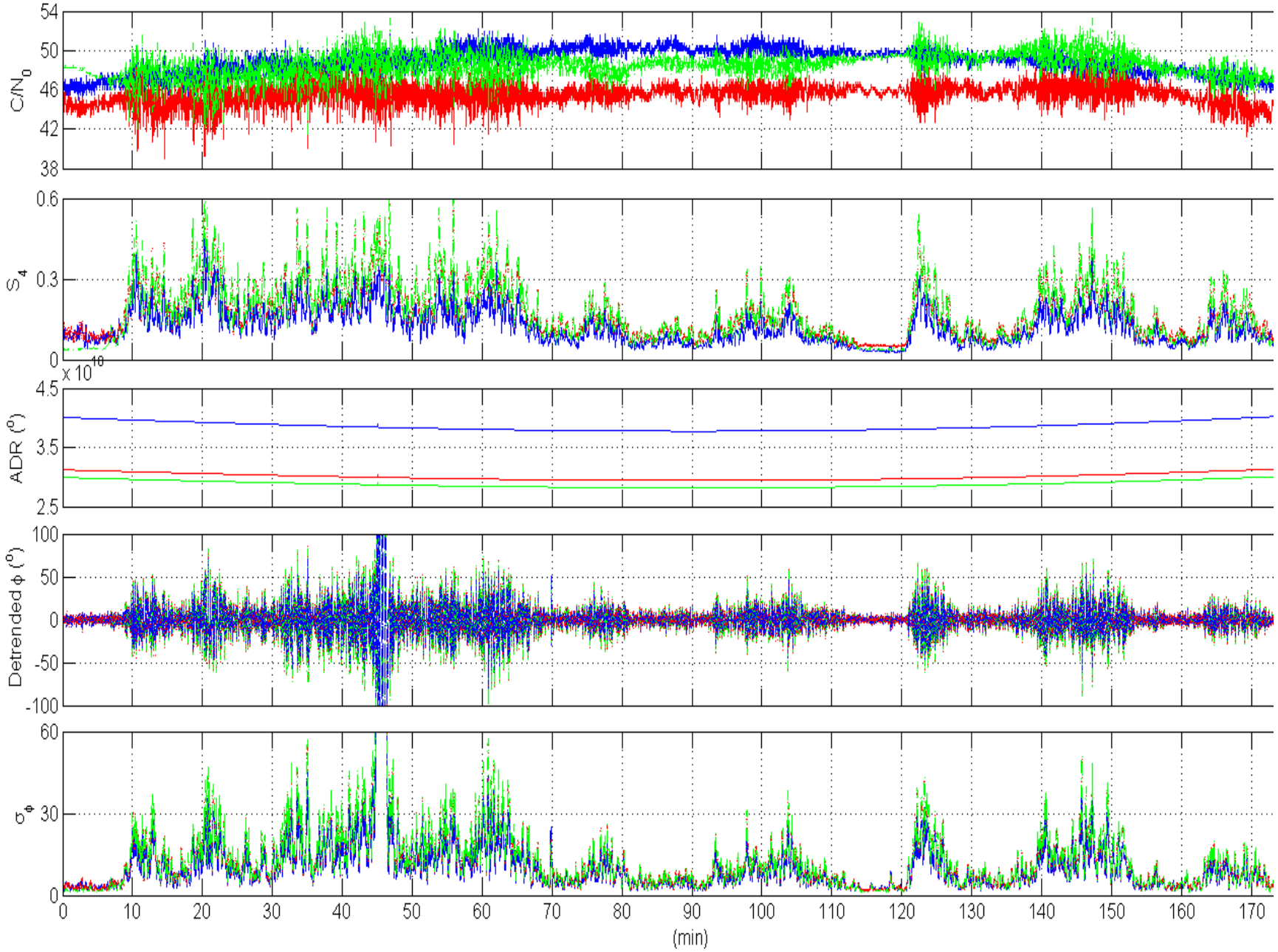

Plasma Velocity Estimation

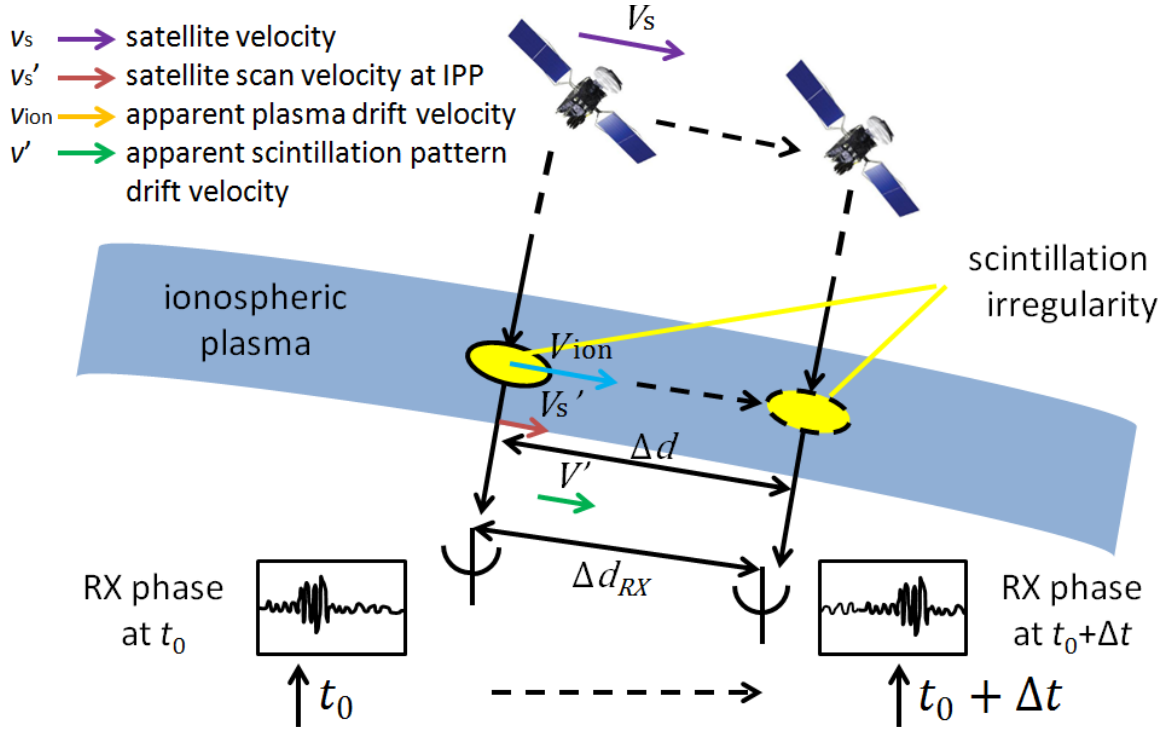

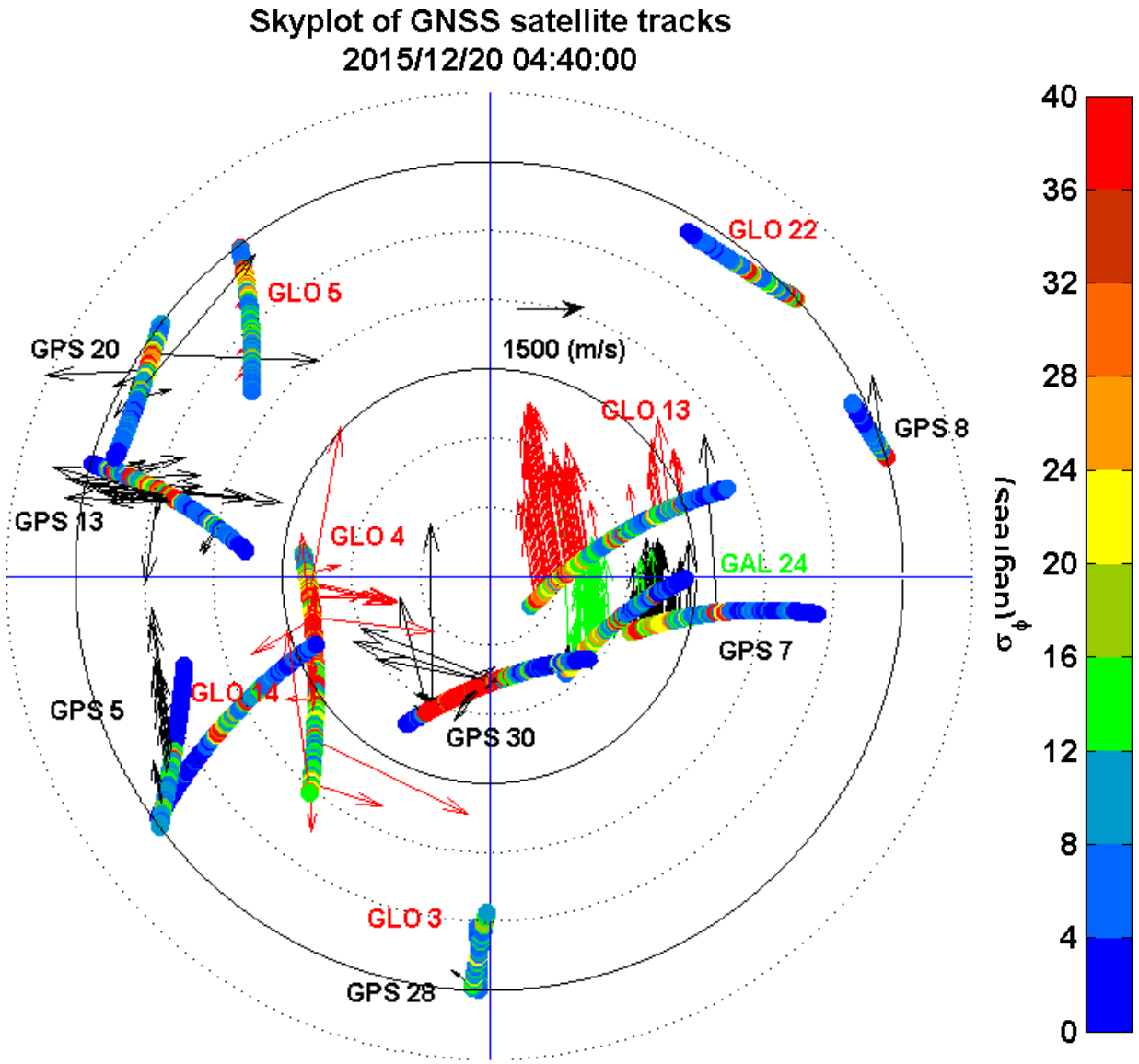

Wang, J., Y. Morton, "Ionospheric irregularity drift velocity estimation using multi-GNSS spaced-receiver array during high latitude phase scintillation," *Radio Sci.*, DOI: 10.1002/2017RS006470, 2018.

Ionosphere TEC and Disturbance Forecasting

(Shi et al., 2015)

Machine Learning Forecast Framework Using ConvLSTM:

(Convolutional Long Short-Term Memory)

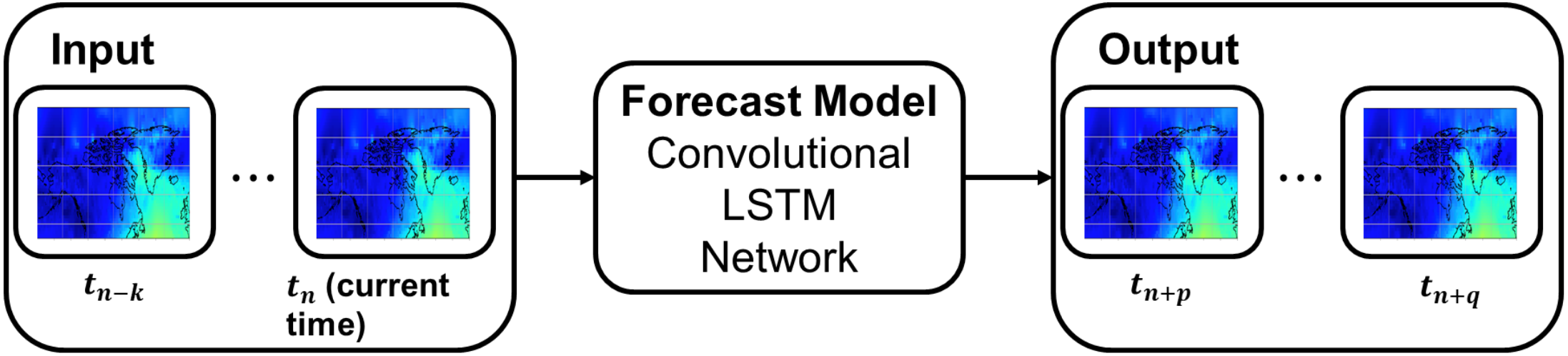

Input/Output	TEC Map: Background Ionosphere
	ROTI Map: Ionosphere Disturbances

Ionosphere Disturbance Forecasting with Ground GNSS Networks

GNSS Receivers **IPP** **Raw ROTI** **Interpreted ROTI**

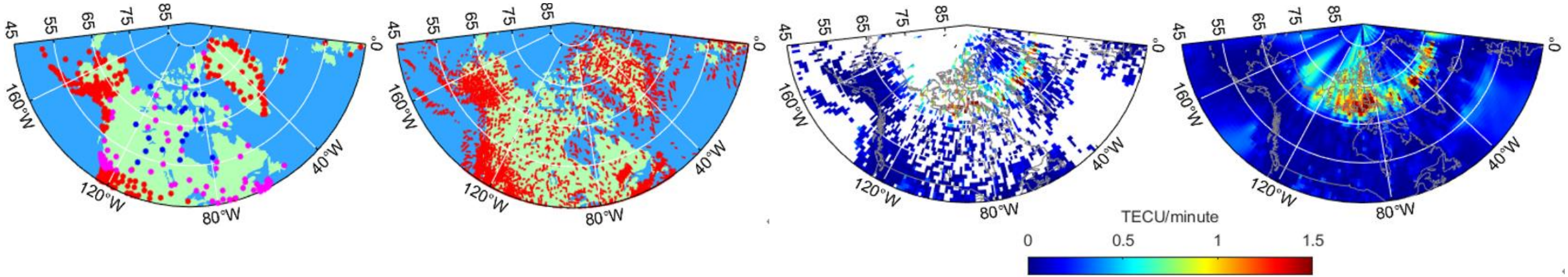

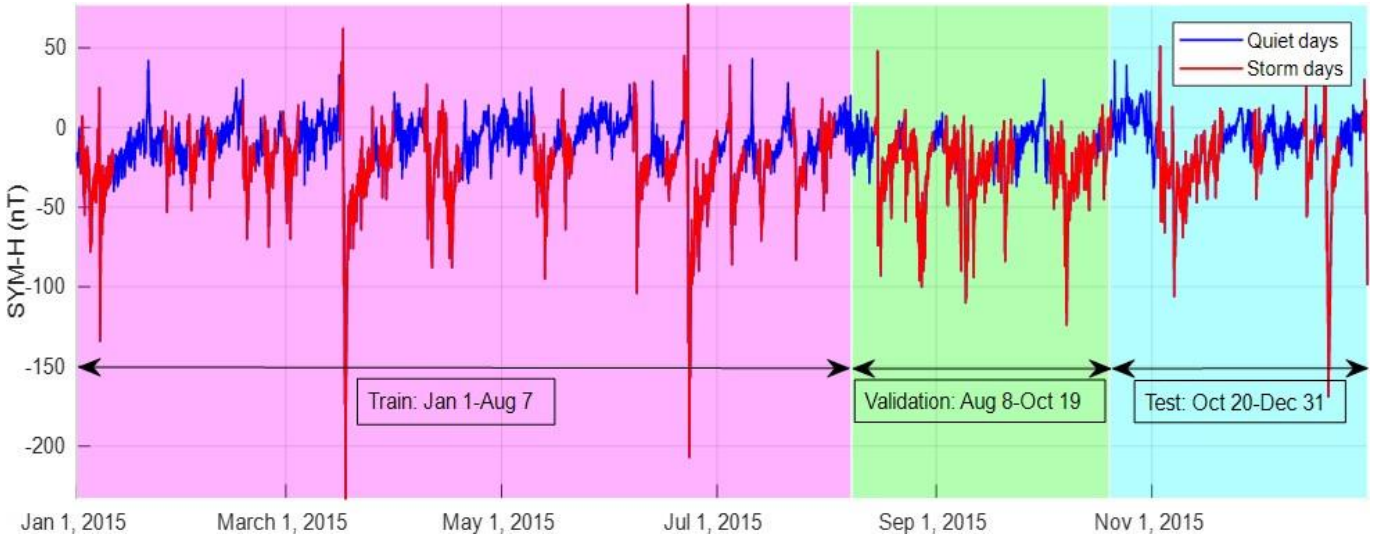

- Lead time steps: 10 minutes
- Resolution: 1° Latitude by 1° Longitude
- Select data of storm days with SYM-H index < -40 nT

Ionosphere Disturbance Forecasting Results

Ionosphere Disturbance Forecast Results:

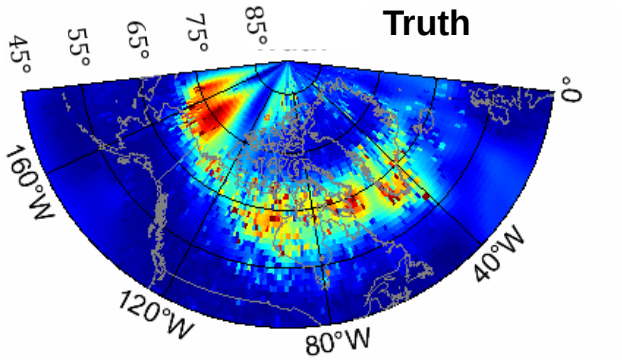

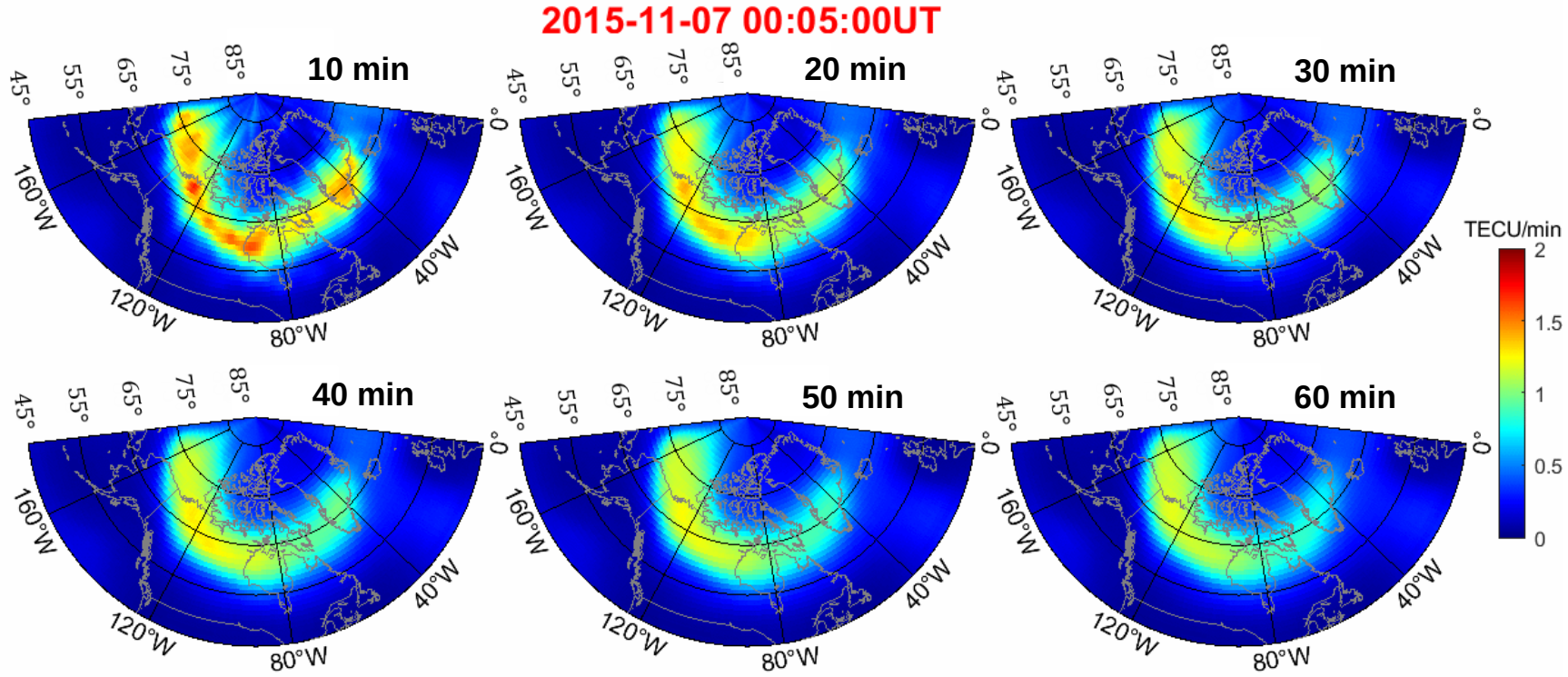

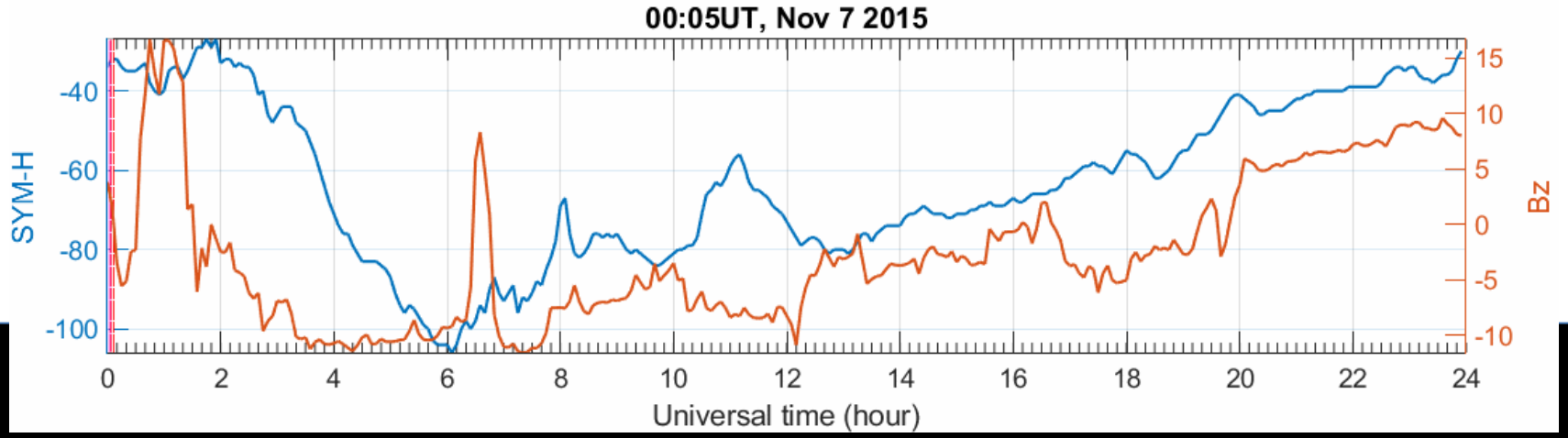

(Liu et al., 2021)

Outline

- Overview of ionosphere observation approaches
- GNSS network-based ionosphere observation and monitoring
- **GNSS space-based ionosphere observations**

Filling the Data Gap: LEO Satellite-Based Observations

GNSS Radio Occultation (GNSS-RO)

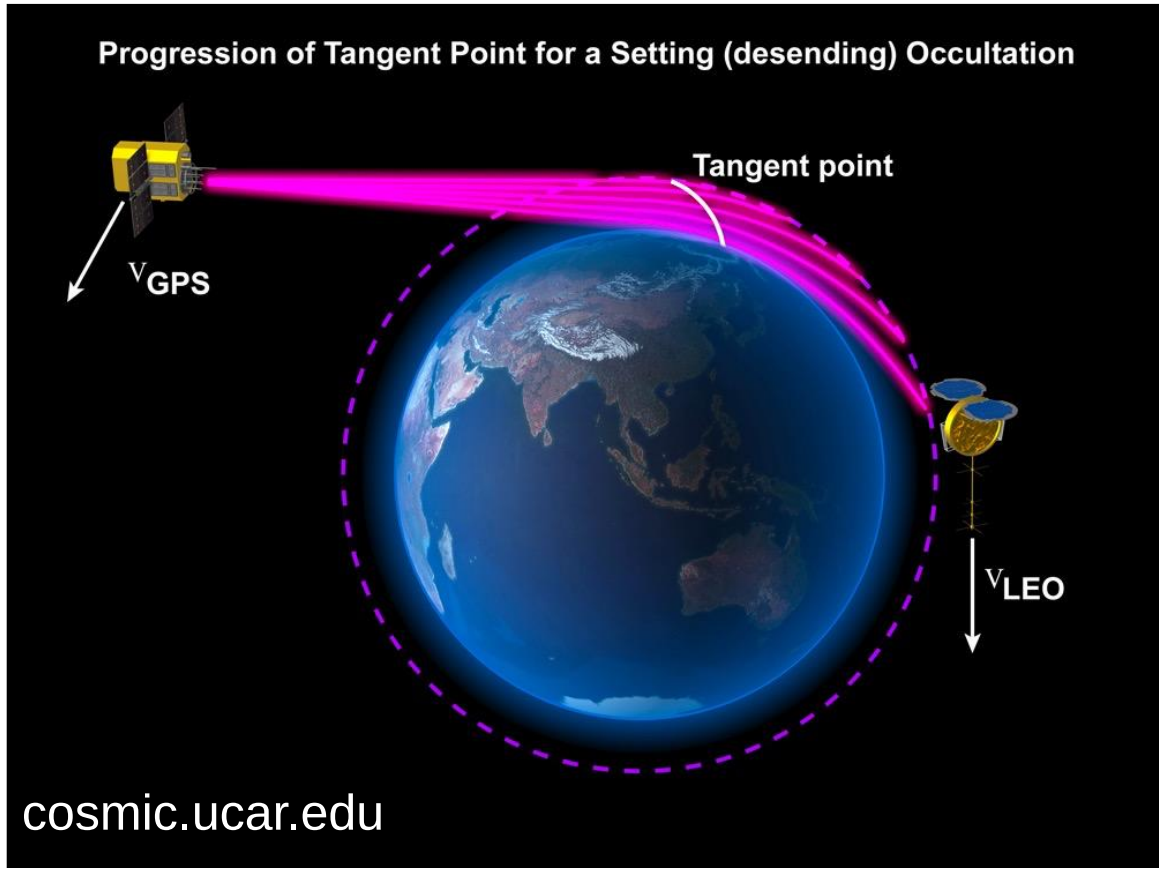

GNSS Reflectometry (GNSS-R)

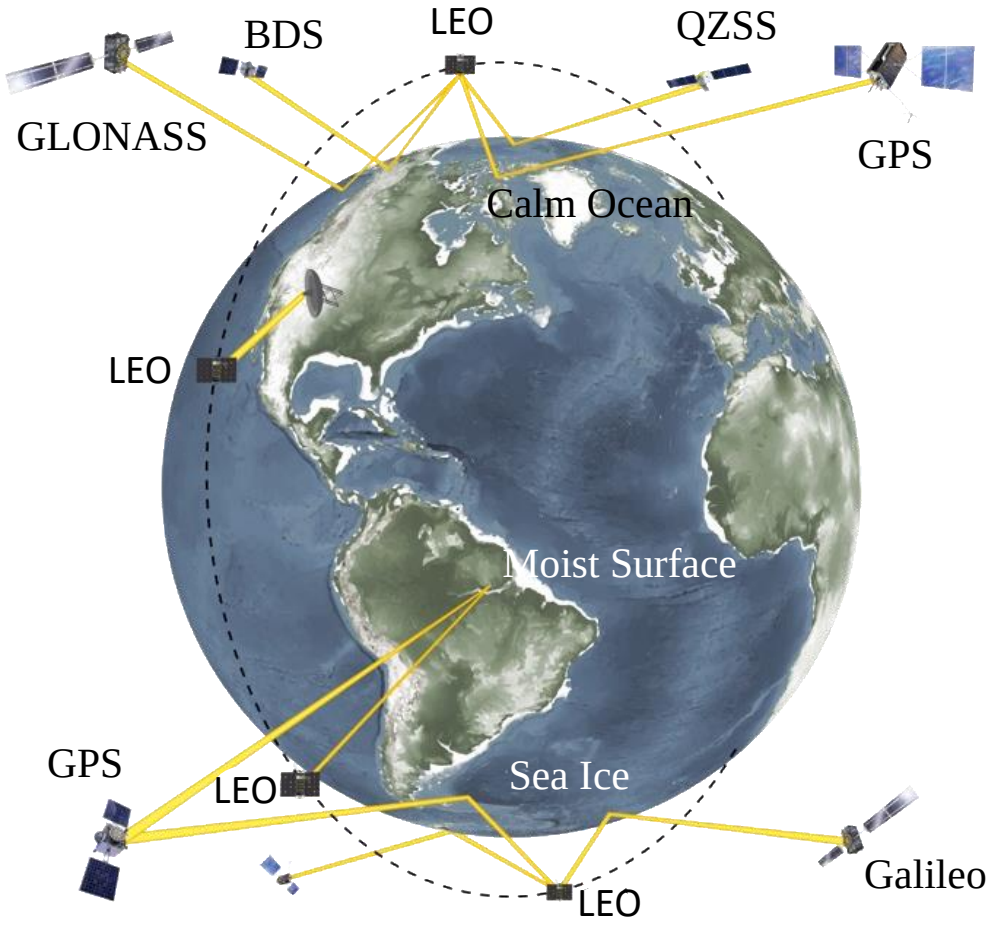

GNSS-RO

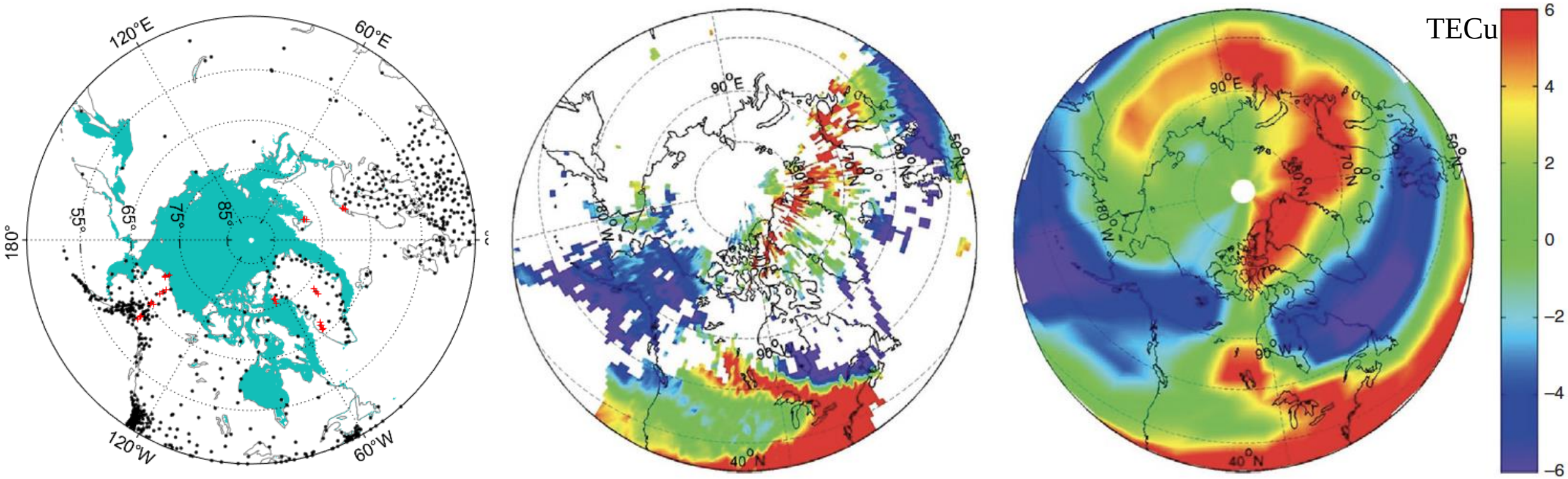

Yue, X., Wan, W., Liu, L., Liu, J., Zhang, S., Schreiner, W. S., ... & Hu, L. (2016). Mapping the conjugate and corotating storm-enhanced density during 17 March 2013 storm through data assimilation. Journal of Geophysical Research: Space Physics, 121(12), 12-202.

GNSS RO Ionosphere Retrieval

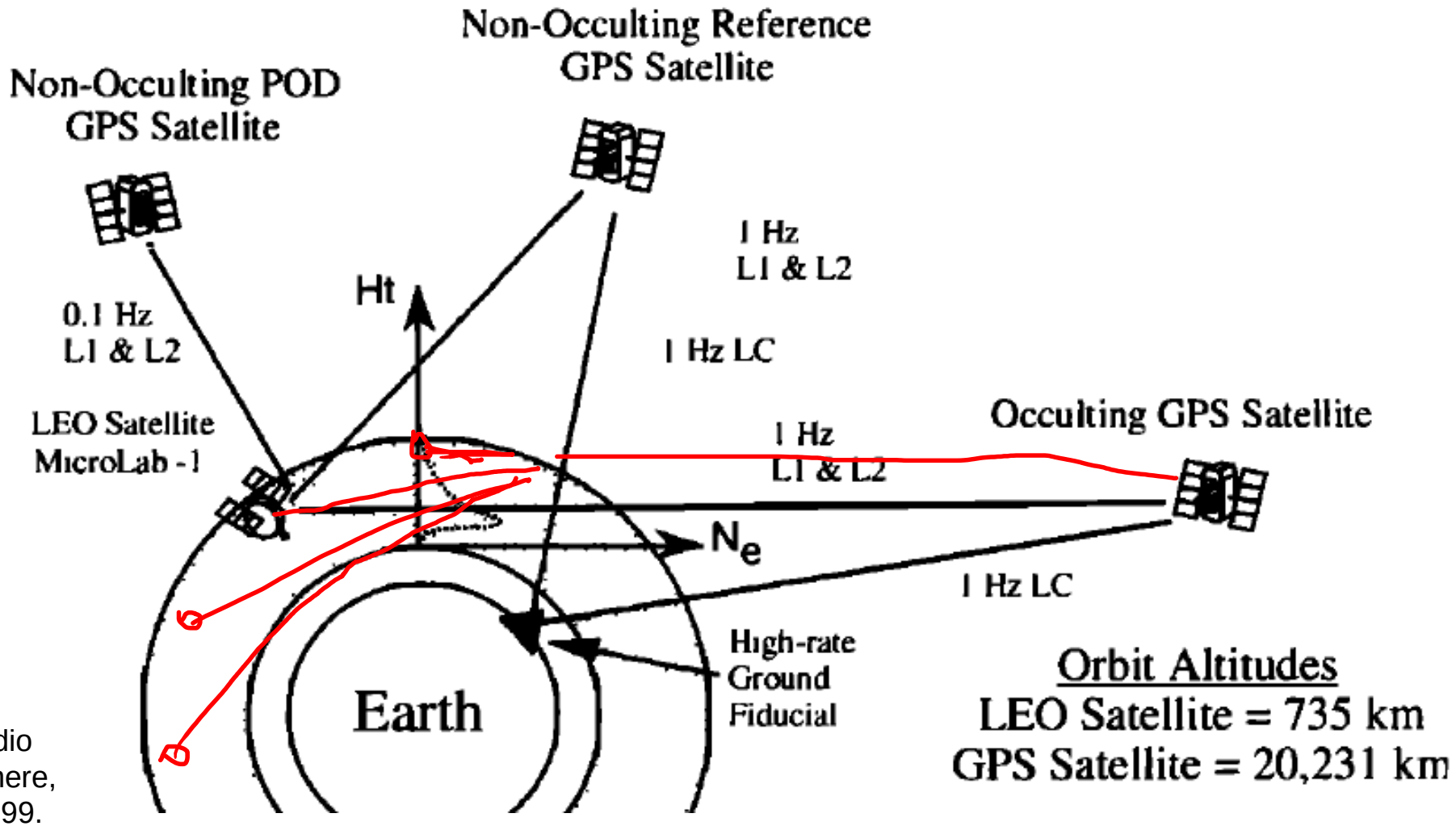

Schreiner et al., GPS/MET Radio Occultation data in the ionosphere, Radio Scie., 34(4):949-966, 1999.

GNSS-RO TEC Retrieval

$$TEC \approx \frac{1}{\beta}\Delta\phi_{12} + \Delta B_{12}$$

$$\frac{1}{\beta} = \frac{1}{40.3}\frac{f_1^2 f_2^2}{f_2^2 - f_1^2}$$

How to calibrate/estimate bias?

- GNSS satellite bias: use ground receiver network estimations, IGS products
- LEO satellite receiver bias:
  - Find geometries that tend to result in minimum TEC along a raypath and use climatological models of ionosphere to estimate the small Ne and TEC in the region. Example: at high latitudes where the ray path traverses regions of open magnetic fields near the poles.
  - Set TEC to 0 along minimum TEC ray path
  - Rely on receiver built-in calibration mechanism

Ionosphere Ne Profile Retrieval

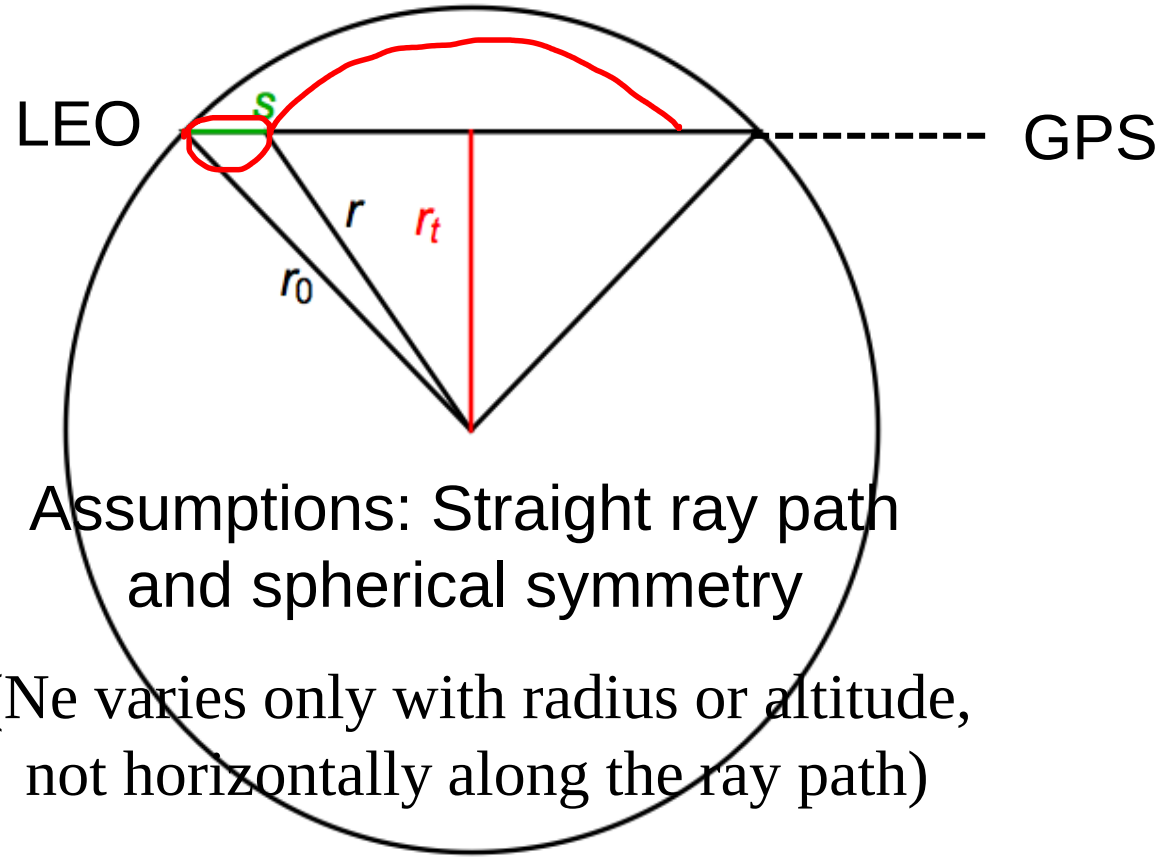

Assumptions: Straight ray path and spherical symmetry

(Ne varies only with radius or altitude, not horizontally along the ray path)

$$TEC = \int_{raypath} N_e(s)ds$$

$$s(r) = \sqrt{r_0^2 - r_t^2} - \sqrt{r^2 - r_t^2}$$

$$\frac{ds(r)}{dr} = \frac{r}{\sqrt{r^2 - r_t^2}}$$

$$TEC(r) = 2\int_{r_0}^{r_t} \frac{rN_e(r)}{\sqrt{r^2 - r_t^2}} dr$$

$$N_e(r) = \frac{1}{\pi}\int_{r}^{r_0} \frac{dTEC}{dr_t} \frac{1}{\sqrt{r_t^2 - r^2}} dr_t$$

Mannucci et al., Chapter 31 GNSS Radio Occultation, PNT21, 2020

Ionospheric Observations from GNSS-RO

Ne profiles, TEC, Scintillation

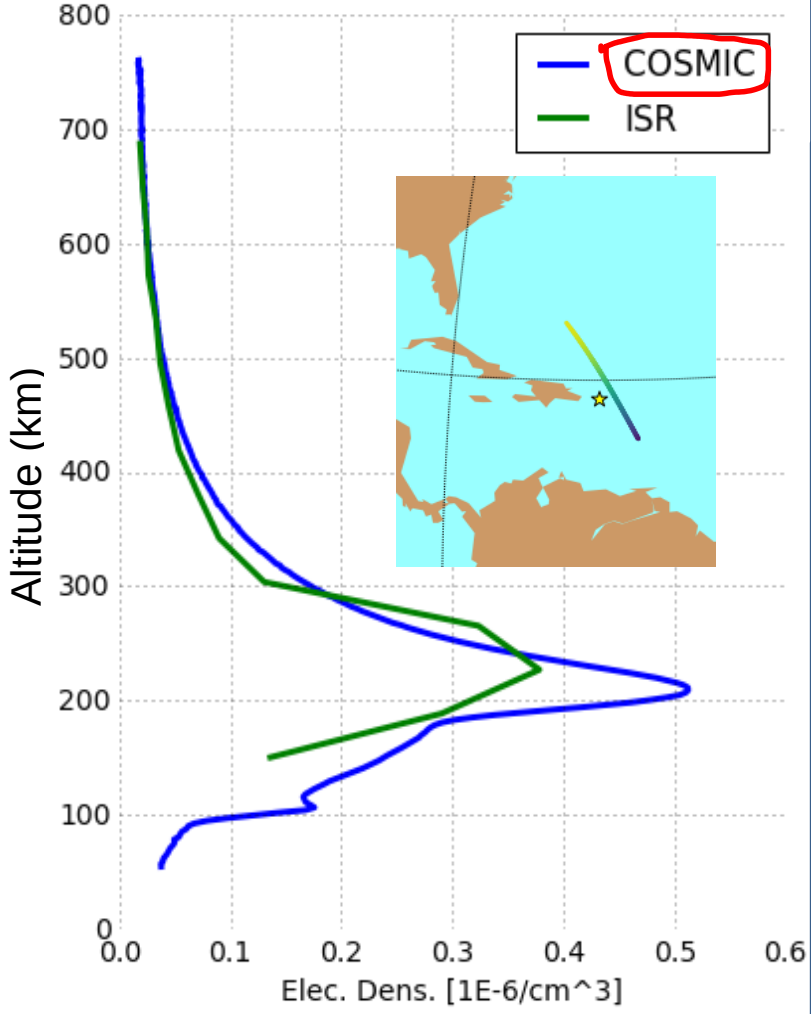

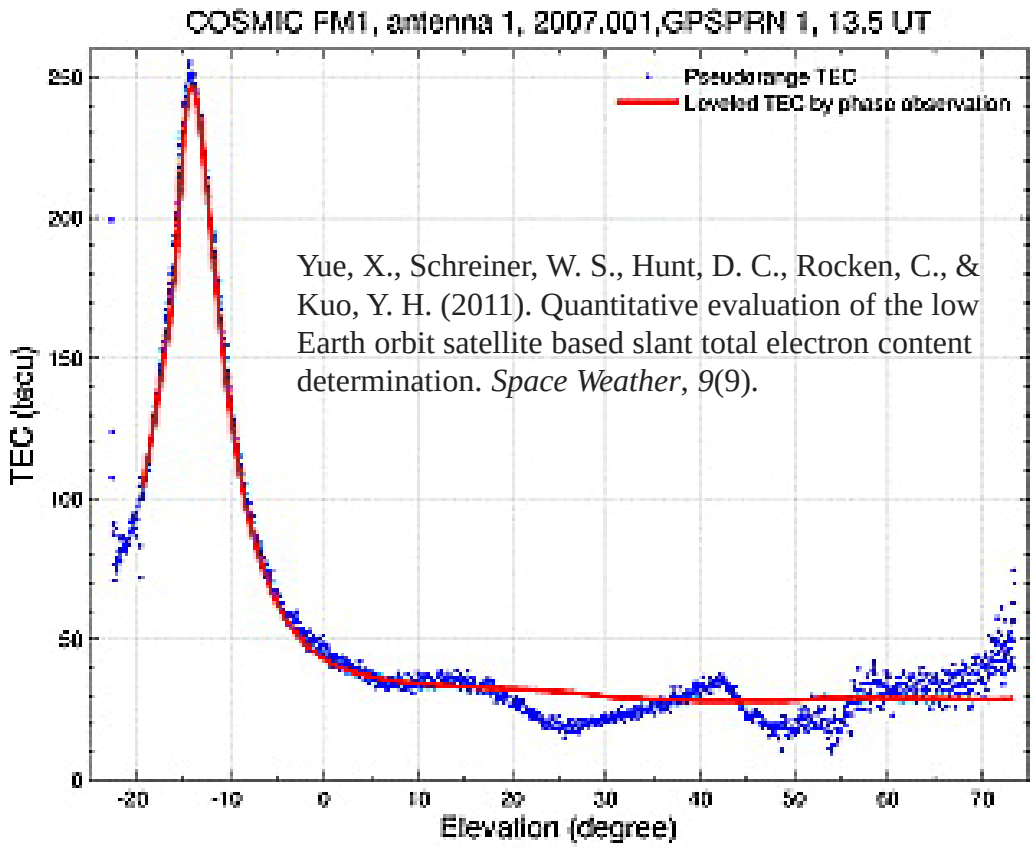

Yue, X., Schreiner, W. S., Hunt, D. C., Rocken, C., & Kuo, Y. H. (2011). Quantitative evaluation of the low Earth orbit satellite based slant total electron content determination. *Space Weather*, *9*(9).

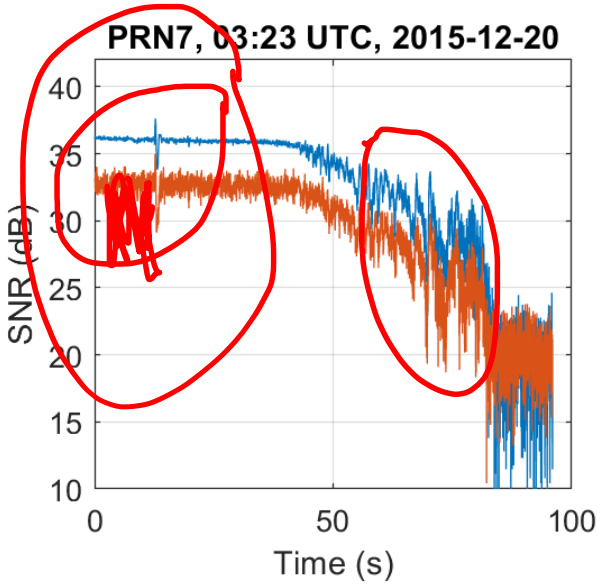

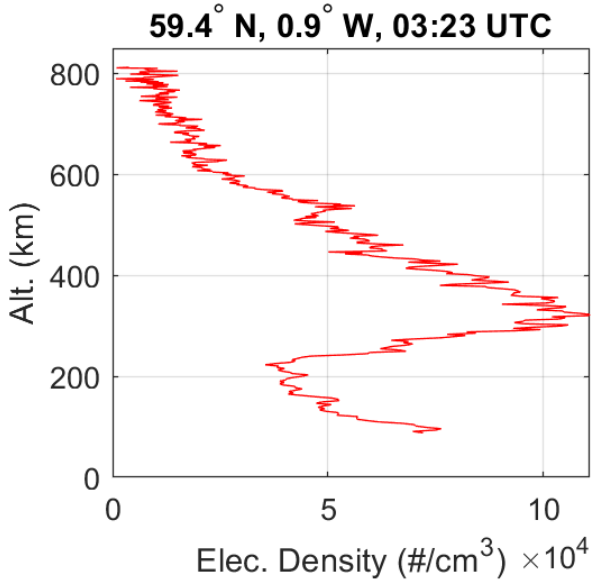

GNSS-R Phase-Delay Altimetry

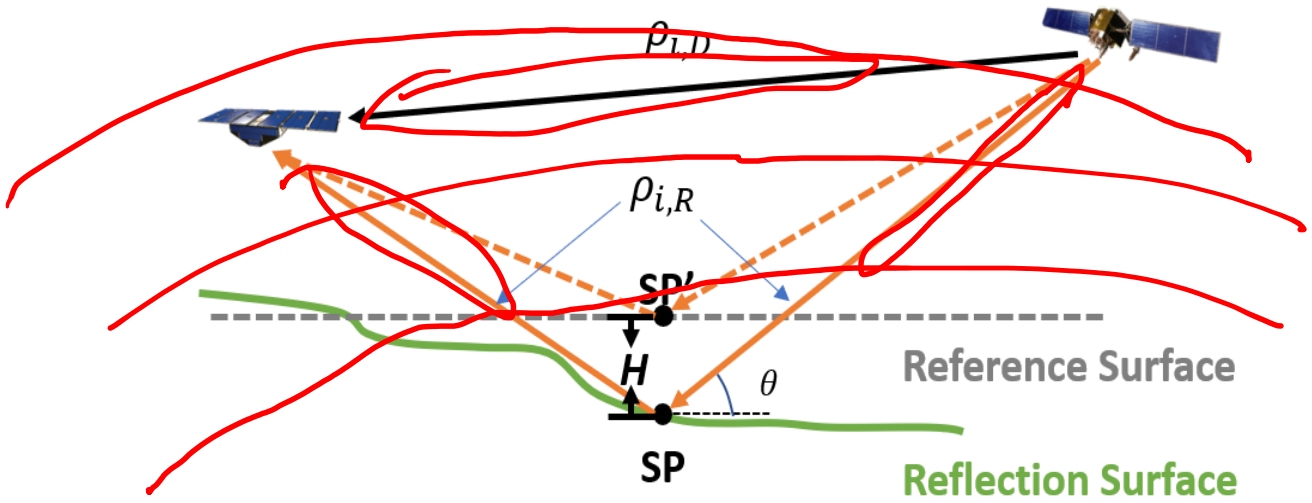

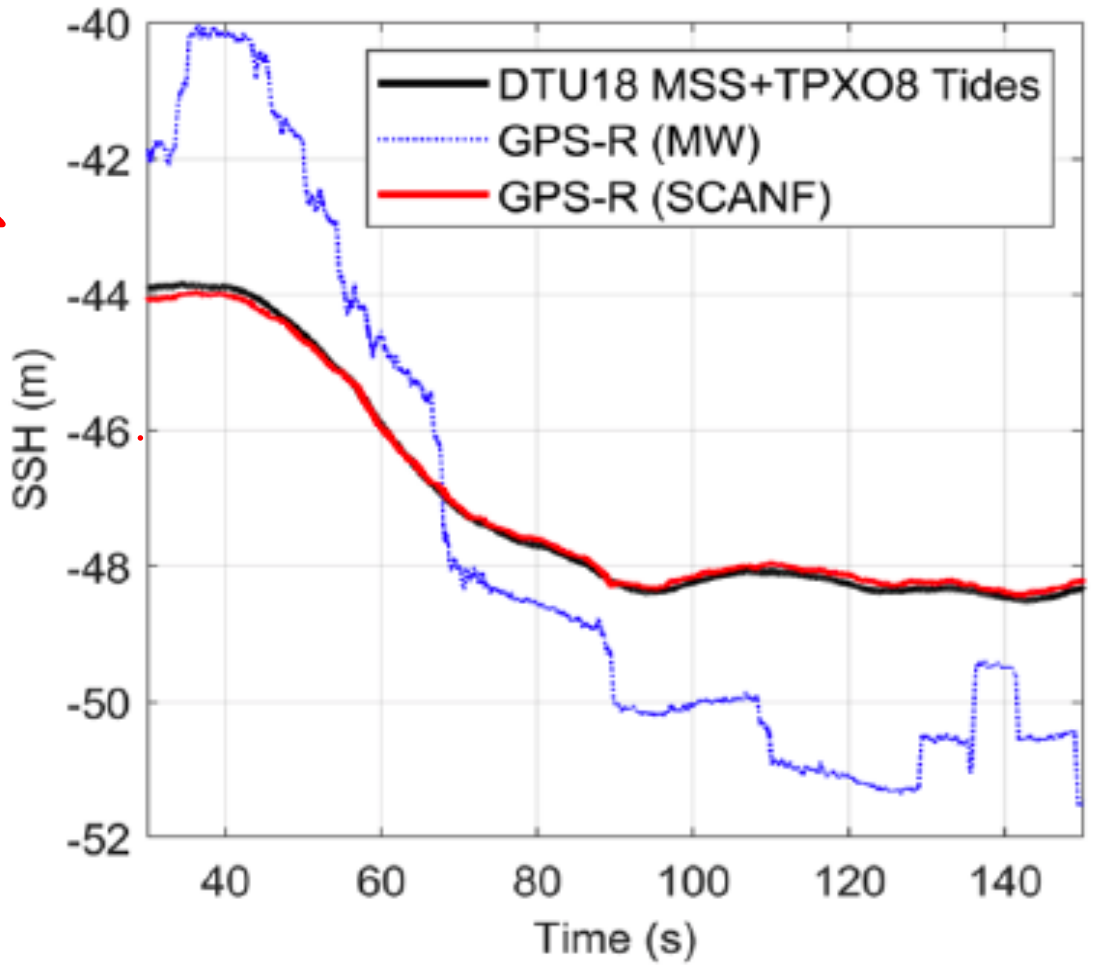

Wang, Y., Y. Morton, "Coherent GNSS reflection signal processing for high-precision and high-resolution spaceborne applications," *IEEE Trans. Geosci. Remote Sensing*, doi:10.1109/TGRS.2020.2993804, *2021*.

Arctic and Antarctic: High Rate Coherent Reflections

42% over sea ice. 75% over 1st year ice

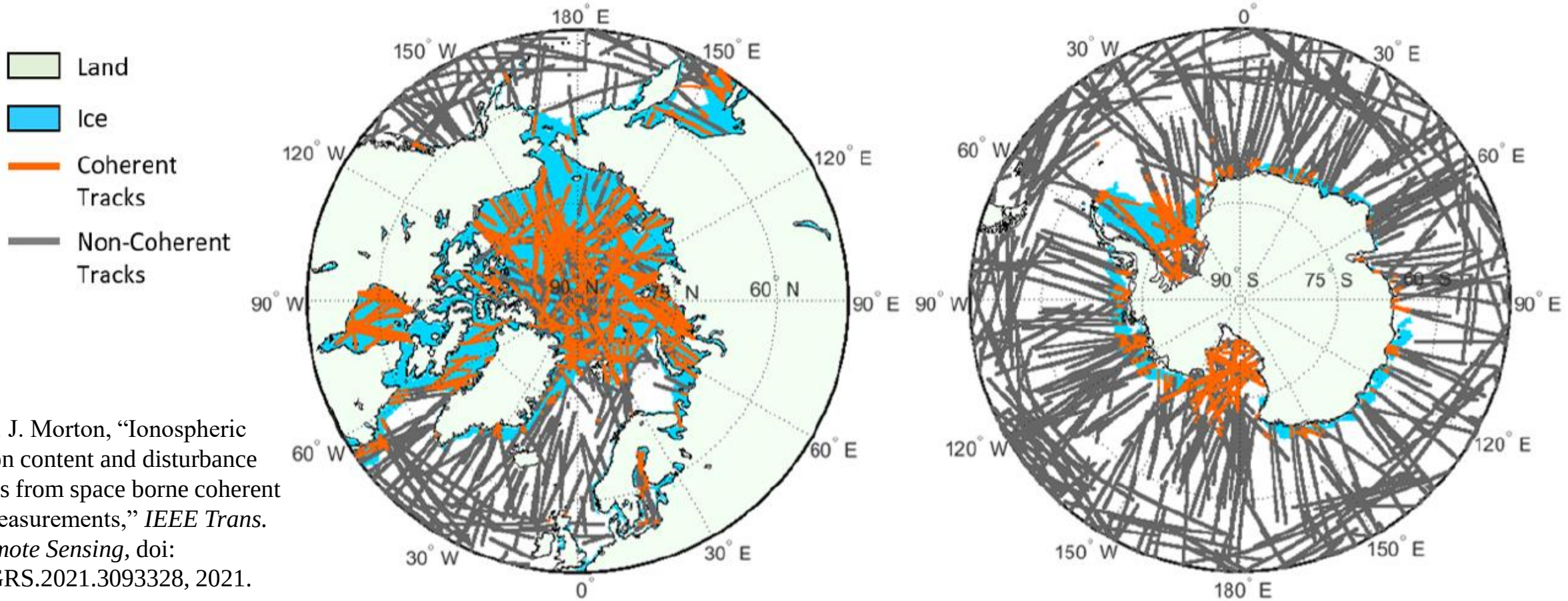

Wang, Y., Y. J. Morton, "Ionospheric total electron content and disturbance observations from space borne coherent GNSS-R measurements," *IEEE Trans. Geosci. Remote Sensing*, doi: 10.1109/TGRS.2021.3093328, 2021.

Example TEC Retrieval from Spire Data: Kara Sea

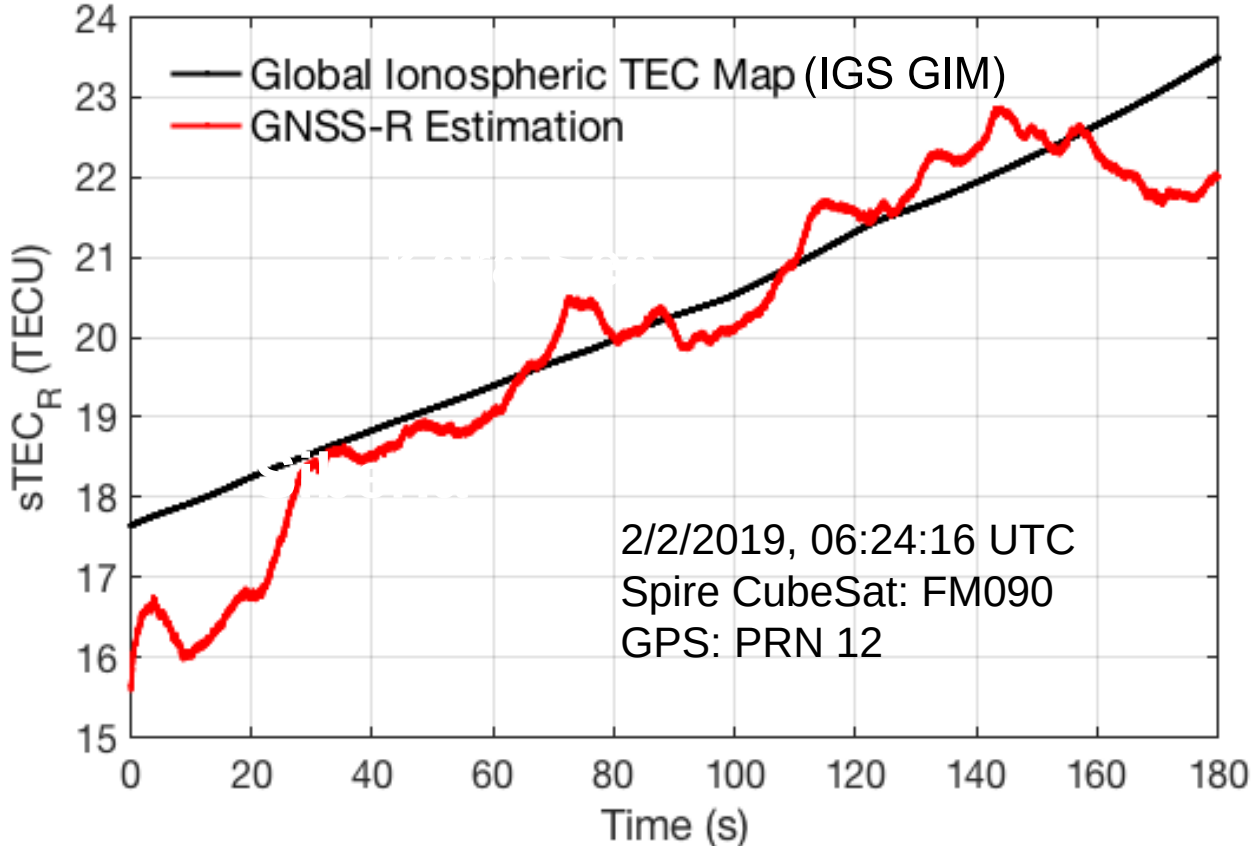

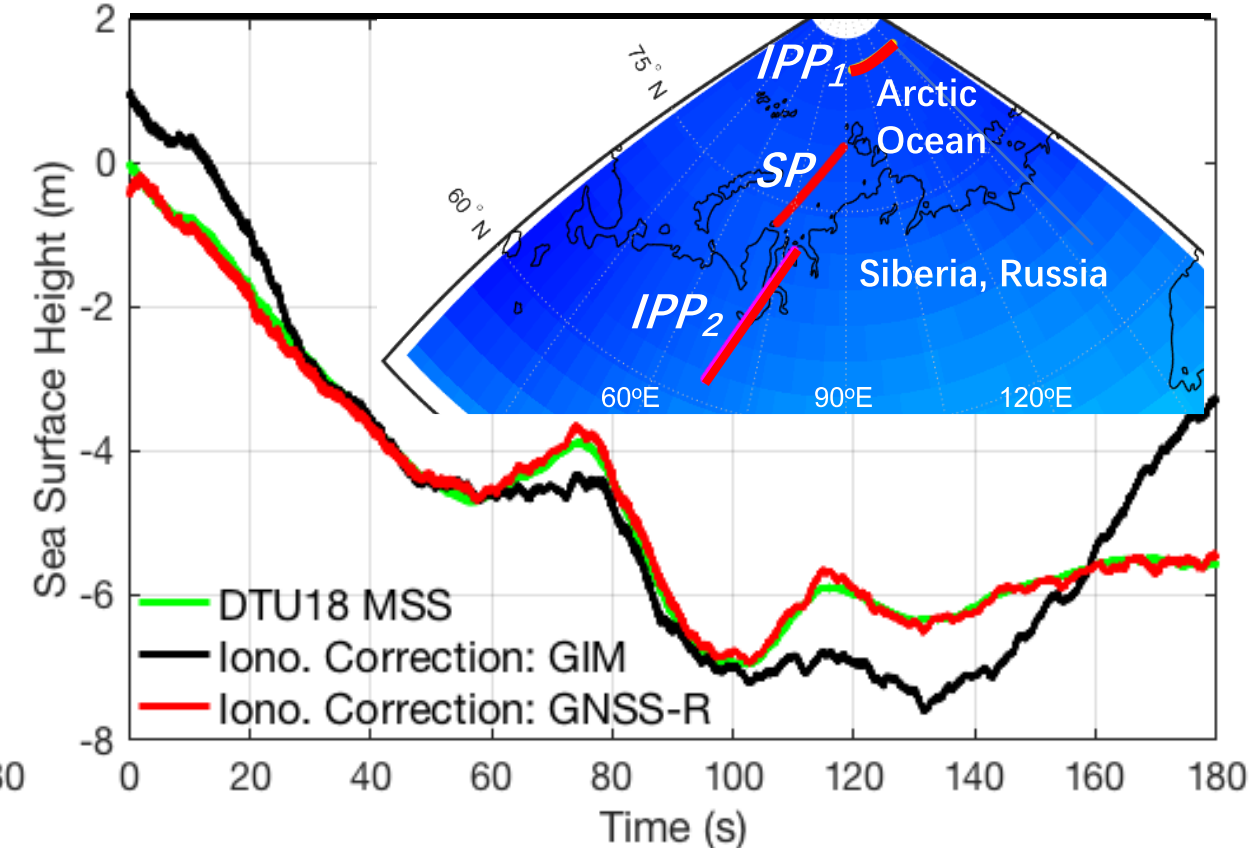

Wang, Y., Y. J. Morton, "Ionospheric total electron content and disturbance observations from space borne coherent GNSS-R measurements," *IEEE Trans. Geosci. Remote Sensing*, doi: 10.1109/TGRS.2021.3093328, 2021.

Ionosphere Structure Observation GNSS-R

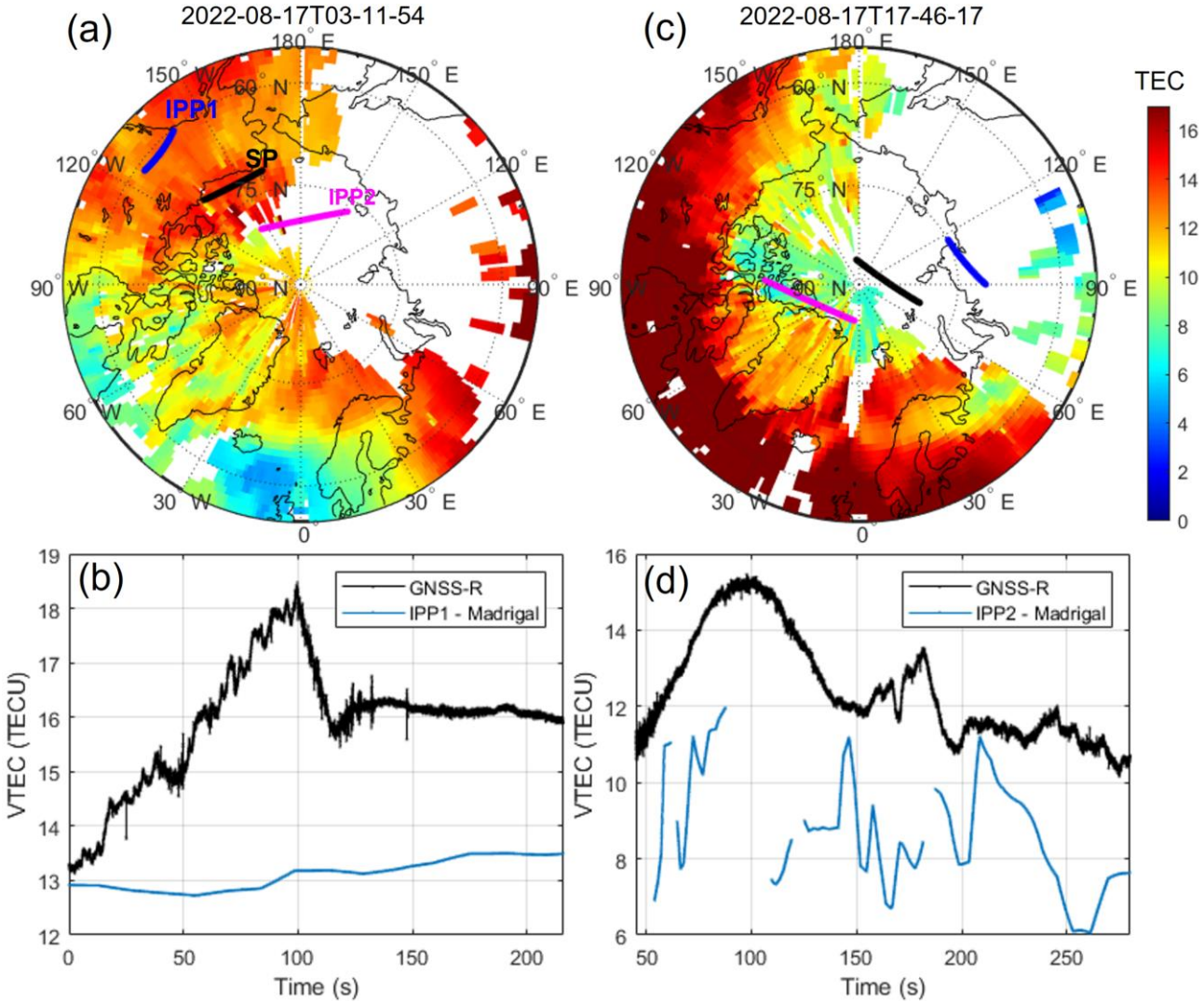

GNSS-R Monitoring Ionospheric Disturbances